1-1-2010

Recent advances in the application of vertical drains and vacuum preloading in soft soil stabilisation

Buddhima Indraratna
University of Wollongong, indra@uow.edu.au

RECENT ADVANCES IN THE APPLICATION OF VERTICAL DRAINS AND VACUUM PRELOADING IN SOFT SOIL STABILISATION

Buddhima Indraratna
Professor and Head, School of Civil, Mining and Environmental Engineering,
Director, Centre for Geomechanics and Railway Engineering
Faculty of Engineering, University of Wollongong, Wollongong City, NSW 2522, Australia

SUMMARY

Much of the world's essential infrastructure is built along congested coastal belts that are composed of highly compressible and weak soils up to significant depths. Soft alluvial and marine clay deposits have very low bearing capacity and excessive settlement characteristics, with obvious design and maintenance implications on tall structures and large commercial buildings, as well as port and transport infrastructure. Stabilising these soft soils before commencing construction is essential for both long term and short term stability. Pre-construction consolidation of soft soils through the application of a surcharge load alone often takes too long, apart from which, the load required to achieve more than 90% consolidation of these mostly low lying, permeable, and very thick clay deposits can be excessively high over a prolonged period. A system of vertical drains combined with vacuum pressure and surcharge preloading has become an attractive ground improvement alternative in terms of both cost and effectiveness. This technique accelerates consolidation by promoting rapid radial flow which decreases the excess pore-pressure while increasing the effective stress.

Over the past 15 years, the Author and his co-workers have developed numerous experimental, analytical and numerical approaches that simulate the mechanics of prefabricated vertical drains (PVDs) and vacuum preloading, including two-dimensional and three-dimensional analyses, and more comprehensive design methods. These recent techniques have been applied to various real life projects in Australia and Southeast Asia. Some of the new design concepts include the role of overlapping smear zones due to PVD-mandrel penetration, pore pressure prediction based on the elliptical cavity expansion theory, and the rise and fall of pore pressure via PVD under cyclic loads. These recent advances enable greater accuracy in the prediction of excess pore water pressure, and lateral and vertical displacement of the stabilised ground.

This E.H. Davis Memorial Lecture presents an overview of the theoretical and practical developments and salient findings of soft ground improvement via PVDs and vacuum preloading, with applications to selected case studies in Australia, Thailand, and China.

1 INTRODUCTION

The booming population and associated development in coastal and metropolitan areas have necessitated the use of previously undeveloped low lying areas for construction purposes (Indraratna *et al.* 1992). Most of the Australian coastal belt contains very soft clays up to significant depths, especially in Northern Queensland and New South Wales. The low bearing capacity and high compressibility of these deposits affects the long term stability of buildings, roads, rail tracks, and other forms of major infrastructure (Johnson 1970). Therefore, it is imperative to stabilise these soils before commencing construction to prevent unacceptable differential settlement. However, attempts to improve deep bearing strata may not commensurate with the overall cost of the infrastructure (Bo et al. 2003). In the past, various types of vertical drains such as sand drains, sand compaction piles, PVDs (geo-synthetic), stone columns, and gravel piles have commonly been used. Certain types of granular piles and deep stone columns may indeed enhance significantly the intensity of the soil. However, because of the minimum risk of damage to utilities from lateral ground movement and a significant reduction in the price of flexible PVDs over the years, they have often been used more than the original conventional compacted sand drains, gravel piles stone columns etc. Their installation can significantly reduce the preloading period by decreasing the length of the drainage path, sometimes by a factor of 10 or more. More significantly, PVDs can be installed quicker with minimum environmental implications and quarrying requirements.

Preloading (surcharge embankment) is one of the most successful techniques for improving the shear strength of low-lying areas because it loads the ground surface to induce a greater part of the ultimate settlement that it is expected to bear after construction (Richart 1957; Indraratna and Redana 2000; Indraratna *et al.* 2005a). In order to control the development of excess pore pressure, a surcharge embankment is usually raised as a multi-stage exercise, with rest periods between the loading stages (Jamiolkowski *et al.* 1983). Since most compressible low-lying soils have very low permeability and are often thick, a lengthy time period is usually needed to achieve the desired primary degree of consolidation (>95%). In these instances, the height of the surcharge can be excessive

from an economic perspective and stability consolidation (Indraratna *et al.* 1994). One drawback of this surcharge technique is that the preload should be applied for a sufficiently long period, which may at times become impractical due to stringent construction schedules and deadlines. When PVDs combined with surcharge preloading is applied, vertical drains provide a much shorter drainage path in a radial direction, which reduces the required preload period significantly. PVDs are cost effective and can be readily installed in moderate to highly compressible soils (up to 40m deep) that are normally consolidated or lightly over-consolidated. PVDs do not offer particular advantages if installed in heavily over-consolidated clays.

Apart from the method of drainage and PVDs combined with surcharge preloading, vacuum pressure has been used to enhance the efficiency of PVD when a desired degree of consolidation is required over a relatively short time period. Negative pore pressures (suction) distributed along the drains and on the surface of the ground accelerate consolidation, reduce lateral displacement, and increase the effective stress. This allows the height of the surcharge embankment to be reduced to prevent any instability and lateral movement in the soil. Today, PVDs combined with vacuum preloading are used more and more in practical ground improvement all over the world.

This EH Davis memorial lecture includes selected salient aspects of more than 15 years of active research conducted at the University of Wollongong in the area of soft soil stabilisation using PVDs and vacuum preloading: undoubtedly a vital Australian contribution to the field of soft soil improvement worldwide, In addition offering a significant component of higher education training through almost a dozen doctoral studies to date, promoting the advancement of current industry practices in infrastructure development in coastal and low lying areas.

2 PRINCIPLES OF VACUUM CONSOLIDATION

The vacuum preloading method for vertical drains was arguably first introduced in Sweden by Kjellman (1942). Since then, it has been used extensively to accelerate the consolidation of soft ground worldwide, for instance at the Philadelphia International Airport, USA; Tianjin port, China; North South Expressway, Malaysia; Reclamation world in Singapore and Hong Kong, China; Suvarnabhumi Second Bangkok International Airport, Thailand; Balina Bypass NSW and the Port of Brisbane, Queensland in Australia, among many other projects (Holtan, 1965; Choa, 1990; Jacob *et al.*, 1994; Bergado *et al.*, 2002; Chu *et al.*, 2000; Yan and Chu, 2003). When a high surcharge load is needed to achieve the desired undrained shear strength, and this cost becomes substantial due to an excessively high embankment and a long preloading period in order to achieve 95% or more consolidation, the optimum solution is to adapt to a combined vacuum and fill surcharge approach. In very soft clays where a high surcharge embankment cannot be constructed without affecting stability (large lateral movement) or having to work within a tight construction schedule, the application of vacuum pressure is quite often the most appropriate choice.

This PVD coupled system is designed to distribute the vacuum (suction) pressure to deep layers of the subsoil to increase the consolidation rate of reclaimed land and deep estuarine plains (e.g. Indraratna *et al.*, 2005b, Chu *et al.*, 2000). The mechanism for vacuum preloading can be explained by the spring analogy (Fig.1) described by Chu and Yan (2005), where the effective stress increases directly due to the suction (negative) pressure, while the total stress remains the same. This is in the context of conventional case surcharge preloading.

The general characteristics of vacuum preloading compared to conventional preloading are as follows (Qian *et al.*, 1992; Indraratna and Chu, 2005):

- The effective stress related to suction pressure increases isotropically, whereby the corresponding lateral movement is compressive. Consequently, the risk of shear failure can be minimised even at a higher rate of embankment construction, although any 'inward' movement towards the embankment toe should be carefully monitored to avoid excessively high tensile stresses.
- The vacuum head can propagate to a greater depth of subsoil via the PVD system and the suction can propagate beyond the tips of the drain and the boundary of the PVD.
- Assuming on air leaks and depending on the efficiency of the vacuum system used in the field, the volume of surcharge fill can be decreased to achieve the same degree of consolidation.

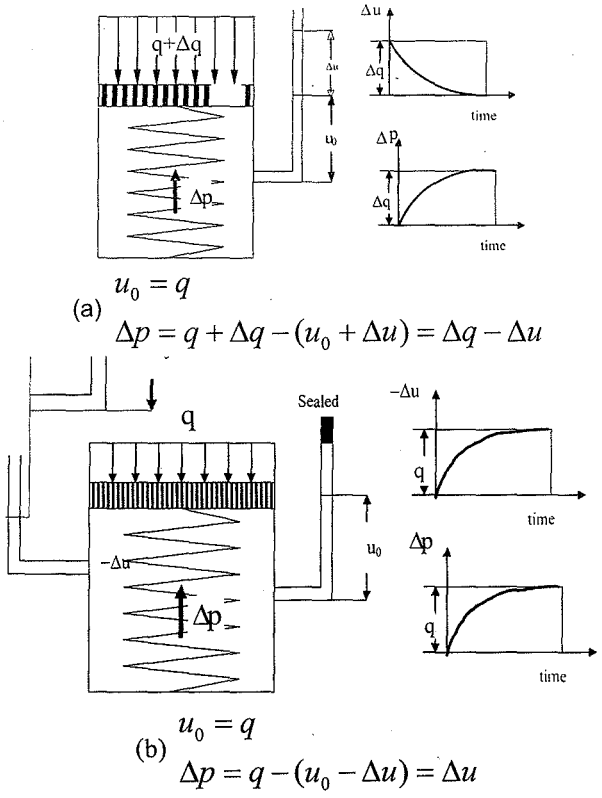

Figure 1: Spring analogy of vacuum consolidation process: (a) under fill surcharge; (b) under vacuum load. (adopted from Chu and Yan, 2005).

- Since the height of the surcharge can be reduced, the maximum excess pore pressure generated by vacuum preloading is less than the conventional surcharge method (Fig. 2).

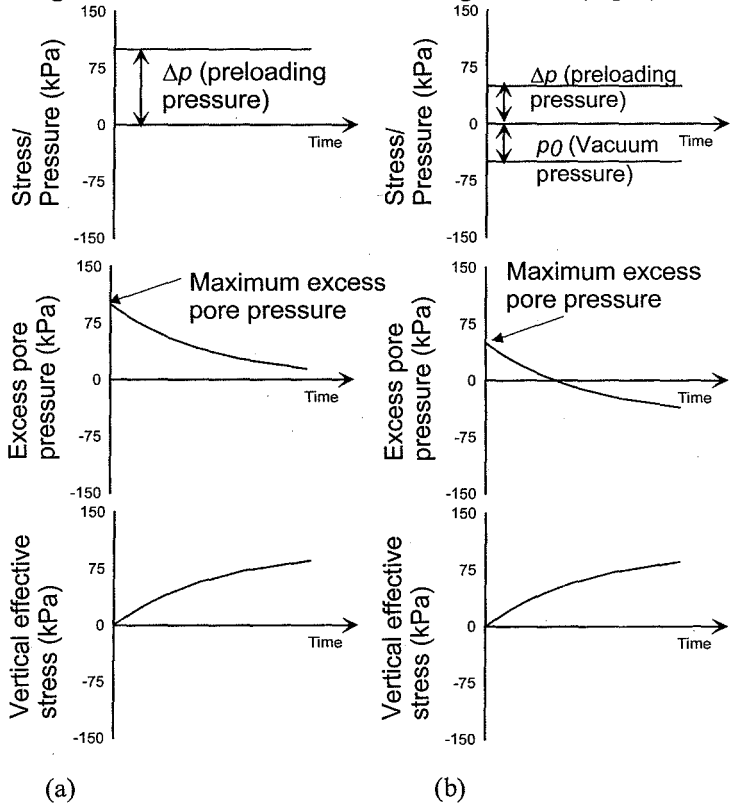

Figure 2: Consolidation process: (a) conventional loading ; (b) idealised vacuum preloading (inspired by Indraratna *et al.*, 2005c).

- With the applied vacuum pressure, the inevitable unsaturated condition at the soil-drain interface may be partially compensated for.
- With field vacuum consolidation, the confining stress applied to a soil element may consist of two parts: (a) vacuum pressure and (b) lateral earth pressure (Chai 2005). Chai *et al.* (2008) demonstrated the possibility of improving clayey deposits by combining the cap-drain with a vacuum and the surface or subsurface soil as a sealing layer, in lieu of an air-tight sheet on the ground surface. However, the efficiency of the method depends on preventing the surface sand from being affected by the pressure from pervious layers of sand and discontinuities in the ground.

It is essential with vacuum assisted preloading that some horizontal drains be placed in transverse and longitudinal directions after installing the sand blanket, in order to uniformly distribute the surface suction. All vertical and lateral drains can then be connected to the edge of a peripheral Bentonite slurry trench, which is normally sealed by an impervious membrane system (Fig. 3a). The trenches can then be filled with water or Bentonite slurry to improve the intact sealing of the membrane around the boundary of the treated zone. The vacuum pumps are then connected to the prefabricated discharge system extending from the trenches (Fig. 3b). The suction head generated by the vacuum pump helps dissipate the excess pore water pressure via the PVDs.

When a reclaimed area has to be sub-divided into a number of sections to facilitate installation of the membrane (e.g. Port of Brisbane), vacuum preloading can only be effectively carried out in one section at a time. Vacuum preloading can become cumbersome over a very large area because the suction head may not be sustained due to the pressure of sand layers, or because it is too close to a marine boundary, in which case a cut off wall will often be used. An alternative method is to apply the vacuum directly to individual PVD with flexible tubes without using a membrane. Here, each PVD is connected directly to the collector drain (Fig. 3b). Unlike the membrane system where an air leak can affect the entire PVD system, in this membraneless system, each drain acts independently. However, installing an extensive tubing system for a large number of PVDs can increase the time and cost of installation (Seah, 2006).

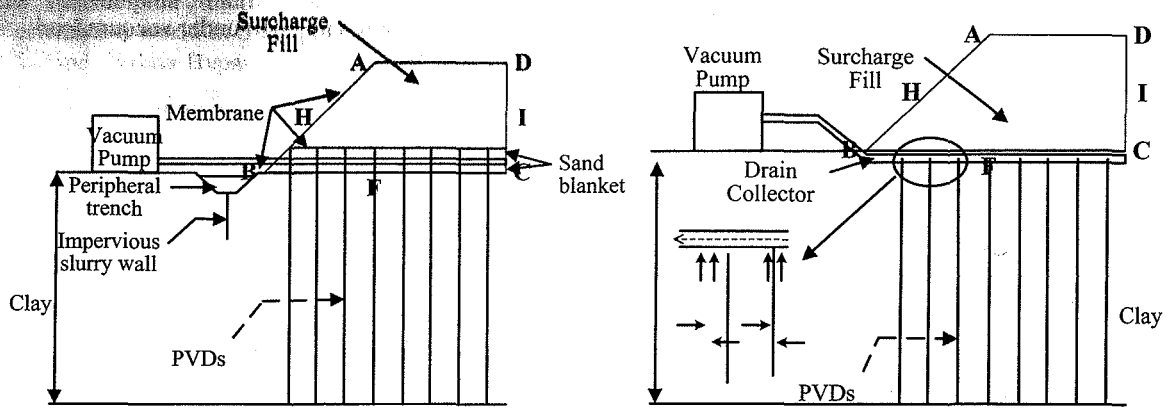

(c)

Figure 3: Vacuum-assisted preloading system: a) membrane system; (b) membraneless system; and (c) vacuum at Port of Brisbane (Indraratna *et al.*, 2005c).

Apart from the obvious inherent characteristics of these two vacuum systems, their effectiveness depends entirely on the properties of the soil, the thickness of the clay, the drain spacing, the type and geometry of PVDs, and the mechanical design and capacity of the vacuum pump. The selection and use of these systems are often based on empirical assessments that are invariably influenced by various aspects of the tender and/or the experience of the contractors, rather than detailed numerical studies. In this section, the analytical solutions to vertical drains incorporating the vacuum preloading of both systems (membrane and membraneless) under time-dependent surcharge loading will be described.

The analytical modelling principles for both systems of the applied vacuum are shown in Fig. 4. The smear zone and well resistance are also considered in both models. The general solutions for excess pore water pressure, settlement, and degree of consolidation were derived through the Laplace transform technique. In addition, a time dependent surcharge preloading can be considered in lieu of an instantaneously applied constant load that can simulate neither the construction history of the embankment nor the variation of the applied vacuum pressure. The results elicited the need for correctly determining the permeability of the sand blanket in the membrane system, and the role of any variation in vacuum in the membraneless system. The permeability of the sand blanket can significantly affect overall consolidation in the membrane system.

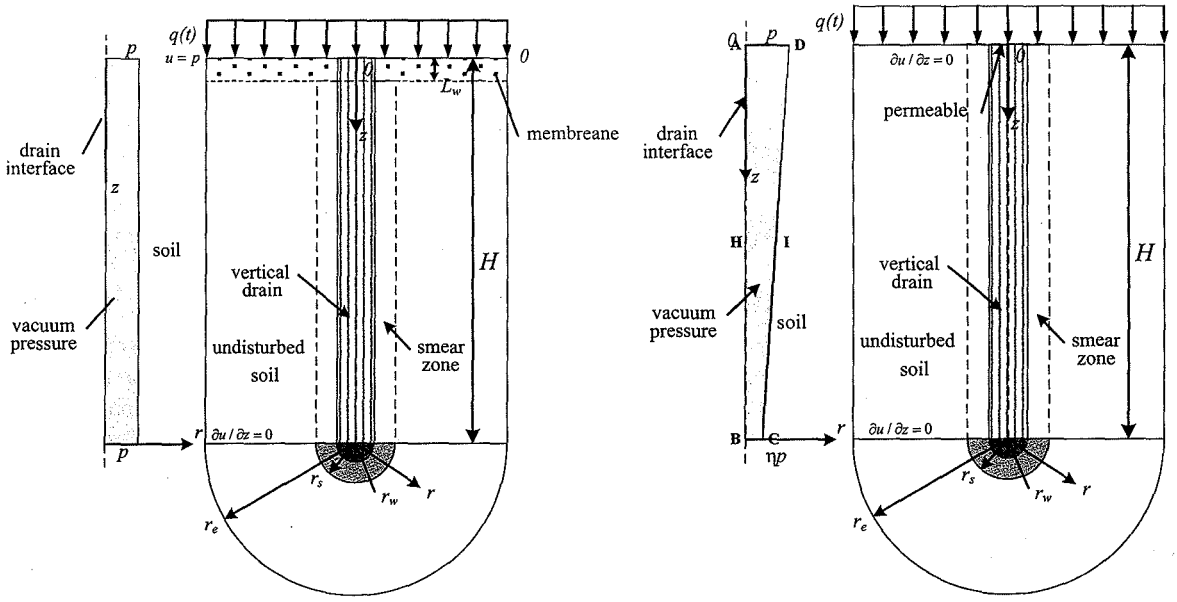

Figure 4: Analysis schemes of unit cell with vertical drain: (a) membrane system; and (b) membrane system.

With the Second Bangkok International Airport, various ground improvement schemes via PVDs with vacuum preloading and conventional surcharge preloading were studied by Indraratna and Redana (2000), and Indraratna *et al.* (2004). Consolidation with only surcharge preloading would take much longer than using vacuum preloading (Fig. 5). The corresponding settlements, excess pore water pressure, and lateral displacement, are presented in Figs. 5 and 6, respectively. As expected, the use of a vacuum pressure increased the rate of excess pore pressure dissipation. This is a direct result of an increased pore pressure gradient towards the drains due to negative pressure (suction) along the length of the drain. The use of sufficient vacuum pressure with properly sealed surface membranes accelerates the preconstruction settlement faster and better than the conventional surcharge preloading method. Moreover, a combination of embankment load with vacuum pressure can reduce the outward lateral displacement (Chai *et al.*, 2005: Indarratna and Redana. 2000).

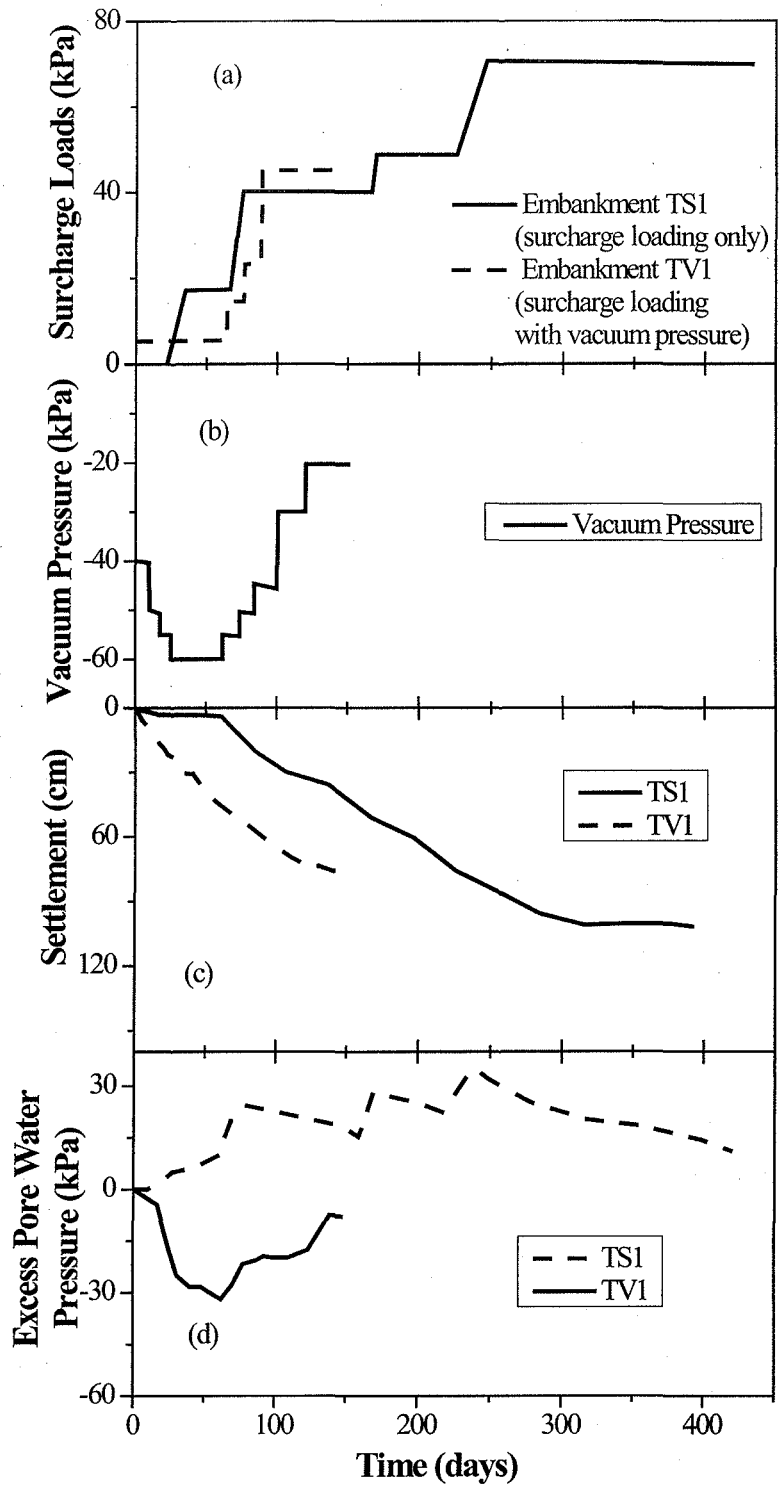

Figure 5: Second Bangkok International Airport (without vacuum pressure): (a) Construction loading history; (b) Surface settlement at the centreline of embankment; (c) Variation of excess pore-water pressure at 8 m depth below ground level at the centreline for embankments (for surcharge only); (d) at 3 m depth below ground level, 0.5 m away from the centreline for embankments (with surcharge and vacuum preloading together) (Indraratna *et al.,* 2000, 2004).

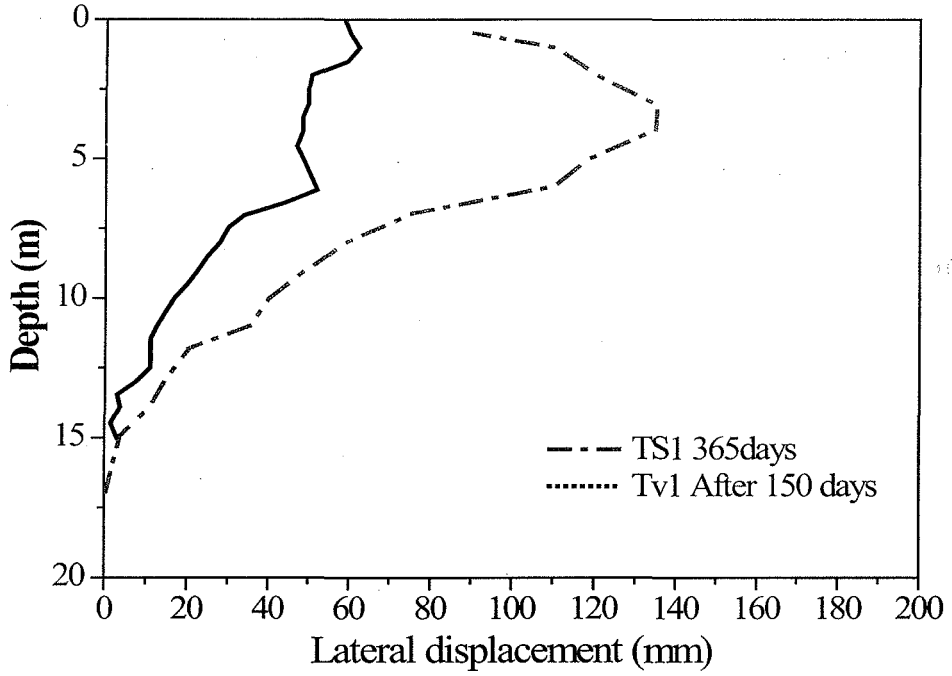

Figure 6: Lateral-displacement profiles 20 m from the centreline of embankments (Indraratna *et al.*, 2000, 2004).

3 VACUUM CONSOLIDATION THEORY

Mohamedelhassan and Shang (2002) developed a combined vacuum and surcharge, load system adopted the one-dimensional Terzaghi's consolidation theory (Figure 7). The mechanism for the combined vacuum and surcharge loading (Fig. 7a) may be determined by the law of superposition (Figs. 7b and 7c). The average of degree of consolidation for combined vacuum and surcharge preloading can then be expressed by:

$$U_{vc} = 1 - \sum_{m=0}^{\infty} \frac{2}{M} \exp^{-M^2 T_{vc}} \quad (1)$$

$$T_{vc} = c_{vc} t / H^2 \quad (2)$$

where T_{vc} is a time factor for combined vacuum and surcharge preloading, and c_{vc} is the coefficient of consolidation for combined vacuum and surcharge preloading.

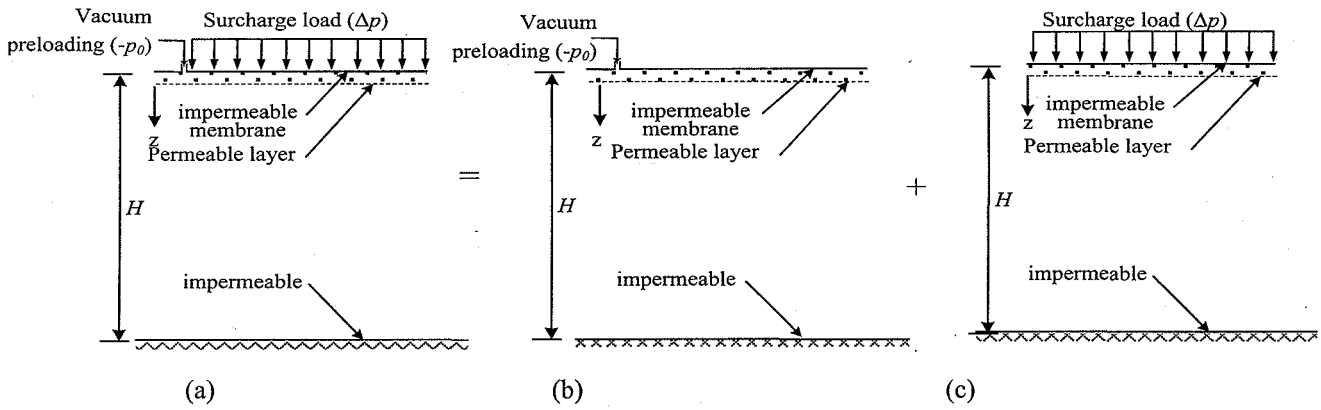

Figure 7: Schematic diagram of vacuum preloading system: (a) vacuum and surcharge combining load; (b) surcharge preloading and (c) vacuum preloading (after Mohamedelhassan and Shang, 2002).

Indraratna *et al.* (2004) showed that when a vacuum is applied in the field through PVDs, the suction head along the length of the drain may decrease with depth, thereby reducing its efficiency. Laboratory measurements taken at a few points along PVDs installed in a large-scale consolidometer at the University of Wollongong clearly indicated that the vacuum propagates immediately, but a gradual reduction in suction may occur along the length of the drain. The rate at which the suction develops in a PVD depends mainly on the length and type of PVD

(core and filter properties). However, some field studies suggest that the suction any develop rapidly even if the PVDs are up to 30 m long (Bo *et al.* 2003; Indraratna *et al.* 2005a).

Indraratna *et al.* (2004, 2005a) proposed a modified radial consolidation theory inspired by laboratory observations to include different distribution patterns of vacuum pressure (Fig. 8). These results indicated that the efficiency of the PVD depended on the magnitude and distribution of the vacuum. In order to quantify the loss of vacuum, a trapezoidal distribution of vacuum pressure along the length of the PVD was assumed.

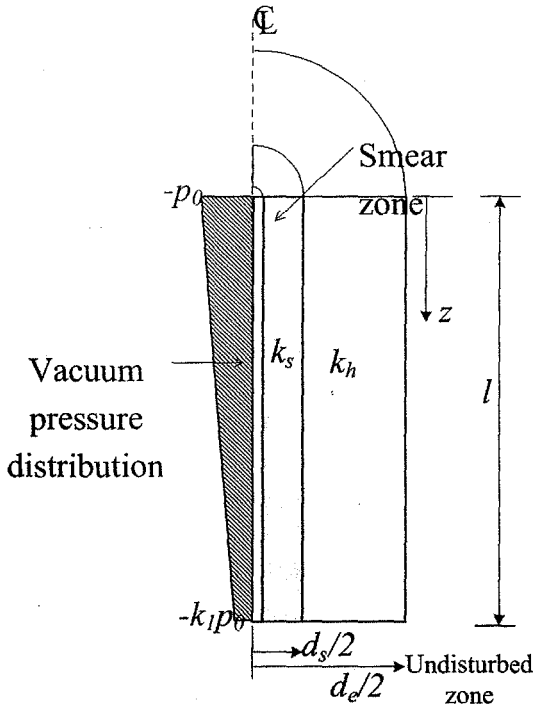

Figure 8: The distribution patterns of vacuum pressure in the vertical directions (after Indraratna *et al.* 2005a).

Based on these assumptions, the average excess pore pressure ratio $(R_u = \Delta p / \bar{u}_0)$ of a soil cylinder for radial drainage that incorporates vacuum preloading can be given by:

$$R_u = \left(1 + \frac{p_0}{\bar{u}_o}\frac{(1+k_1)}{2}\right)\exp\left(-\frac{8T_h}{\mu}\right) - \frac{p_0}{\bar{u}_0}\frac{(1+k_1)}{2} \tag{3}$$

and

$$\mu = \ln\left(\frac{n}{s}\right) + \left(\frac{k_h}{k_s}\right)\ln(s) - 0.75 + \pi z(2l - z)\frac{k_h}{q_w}\left\{1 - \frac{k_h/k_s - 1}{(k_h/k_s)(n/s)^2}\right\} \tag{4}$$

Where, p_0 = the vacuum applied at the top of the drain, k_1 = ratio between the vacuum at the top and bottom of the drain, $\bar{u}_0$ = the initial excess pore water pressure, k_h = the horizontal permeability coefficient of soil in the undisturbed zone, k_s = the horizontal permeability coefficient of soil in the smear zone, T_h = the time factor, n = the ratio d_e/d_w (d_e is the diameter of the equivalent soil cylinder = $2r_e$ and d_w is the diameter of the drain = $2r_w$), s = ratio d_s/d_w (d_s is the diameter of the smear zone = $2r_s$), z = depth, l = the equivalent length of drain, q_w = the well discharge capacity.

4 FACTORS INFLUENCING THE PERFORMANCE OF A VACUUM OR SURCHARGE PRELOADING WITH CONSOLIDATED PVDS

4.1 SMEAR ZONE

Installing vertical drains with a steel mandrel significantly remoulds the subsoil, especially in its immediate vicinity. This disturbed annulus in the smear zone has a reduced lateral permeability and increased compressibility. In varved clays, the finer and more impervious layers are dragged down and smeared over the

more pervious layers which in turn decreases the permeability of the soil near the periphery of the drain. Barron (1948) suggested the concept of reduced permeability by arbitrarily lowering the apparent value of the coefficient of consolidation. Hansbo (1979) included a further explicit smear zone with a reduced permeability near the drain, surrounded by an outer undisturbed zone.

Based on constant but reduced permeability in the smear zone, Jamiolkowski *et al.* (1983) proposed that the diameter of the smear zone (d_s) and the cross section of the mandrel can be related by:

$$d_s = (2.5 \text{ to } 3) \quad d_m \tag{5}$$

In the above, d_m is the diameter of the circle with an area equal to the cross section of the mandrel. Based on the results of Akagi (1979) and Hansbo (1987), the smear zone is often evaluated by the simple expression:

$$d_s = 2d_m \tag{6}$$

Onoue *et al.* (1991) introduced a three zone hypothesis defined by (a) a plastic smear zone close to the drain where the soil is highly remoulded during installation, (b) a plastic zone where the permeability is reduced moderately, and (c) an outer undisturbed zone where the soil is unaffected by installation. For practical purposes, a two-zone approach is generally sufficient.

On the basis of their experimental work, Indraratna and Redana (1998) proposed that the estimated smear zone is at least 3-4 times larger than the cross section of the drain. This proposed relationship was verified using a specially designed large scale consolidometer (the schematic section is shown in Fig. 9. Figure 10 shows the variation of the ratio of horizontal to vertical permeability (k_h/k_v), and the water content along a radial distance from the central drain in the large scale consolidation apparatus (Indraratna and Redana (1998), Sathananthan and Indraratna 2006a, Walker and Indraratna (2006). The radius of the smear zone is about 2.5 times the equivalent radius of the mandrel. The lateral permeability (within the smear zone) is 61%~92% of the outer undisturbed zone, which is similar to Hansbo (1987) and Bergado *et al.* (1991) recommendations. Only recently, Sathananthan *et al.* (2008) used the cavity expansion theory (CET), obeying the modified Cam-clay model, to analyse the extent of the smear zone caused by mandrel driven vertical drains. Their predictions were verified by large scale laboratory tests where the extent of the smear zone was quantified based on (a) response of excess pore pressure generated while driving the steel mandrel, (b) change in lateral permeability, and (c) obvious reduction in the water central towards the content drain.

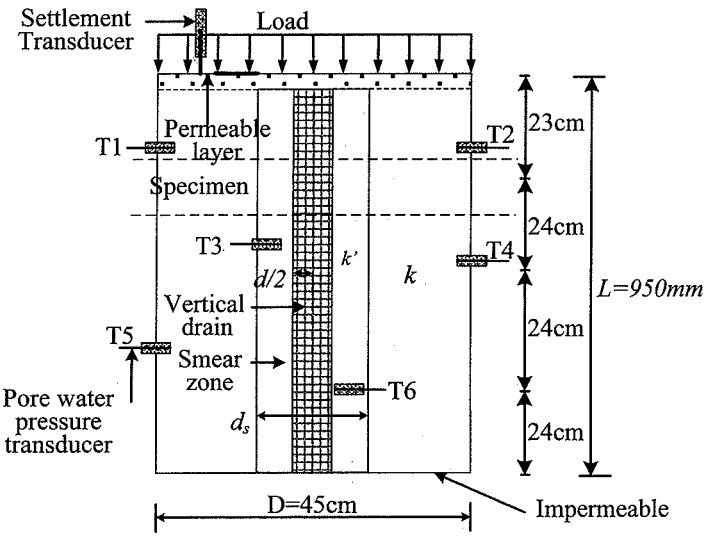

Figure 9: Schematic section of the test equipment showing the central drain and associated smear (after Indraratna and Redana, 1998).

As inspired by field observations, a lower boundary for drain spacing seems to exist, below which there is no discernible increase in the rate of consolidation. Walker and Indraratna (2007) investigated the effect of overlapping smear zones by incorporating a more realistic linear permeability distribution. As shown in Fig. 11, two smear zones will interact when the spacing parameter n is less than the parameter s of the smear zone. With reference to the undisturbed soil properties, a newly modified expression μ_X representing the effect of interacting smear zones can be defined. Figure 12 shows the time required to reach 90% consolidation (t_{90}) for various interacting smear zone configurations. As Figure 12 suggests, a range of drain spacing values exist, across which the time required to reach a certain degree of consolidation does not change. These results are also

in agreement with some observations reported by Saye (2001). This new analytical model for overlapping smear zones provides the basis for selecting the minimum drain spacing, below which the rate of consolidation may decrease. It appears that this radius of minimum influence is 0.6 times the value of the radius of the linear smear zone assumed for non-overlapping smear zones.

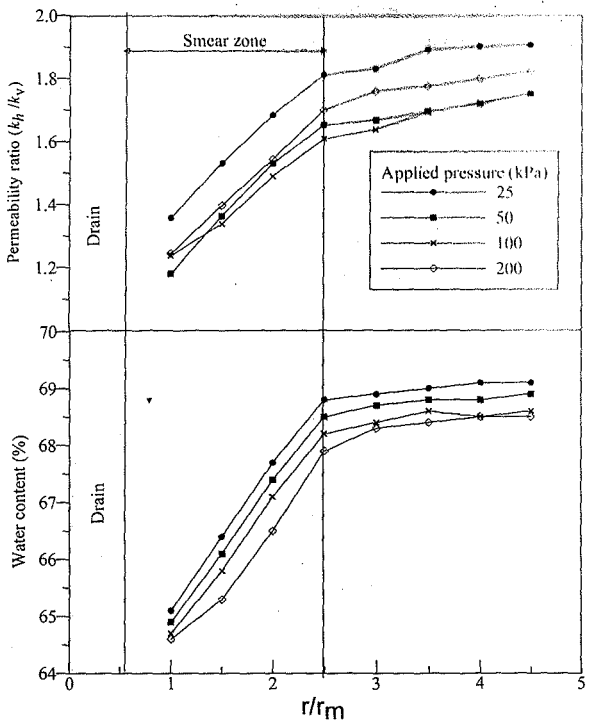

Figure 10: Smear zone determination using: (a) permeability ratio; and (b) water content (After Sathananthan and Indraratna, 2006a).

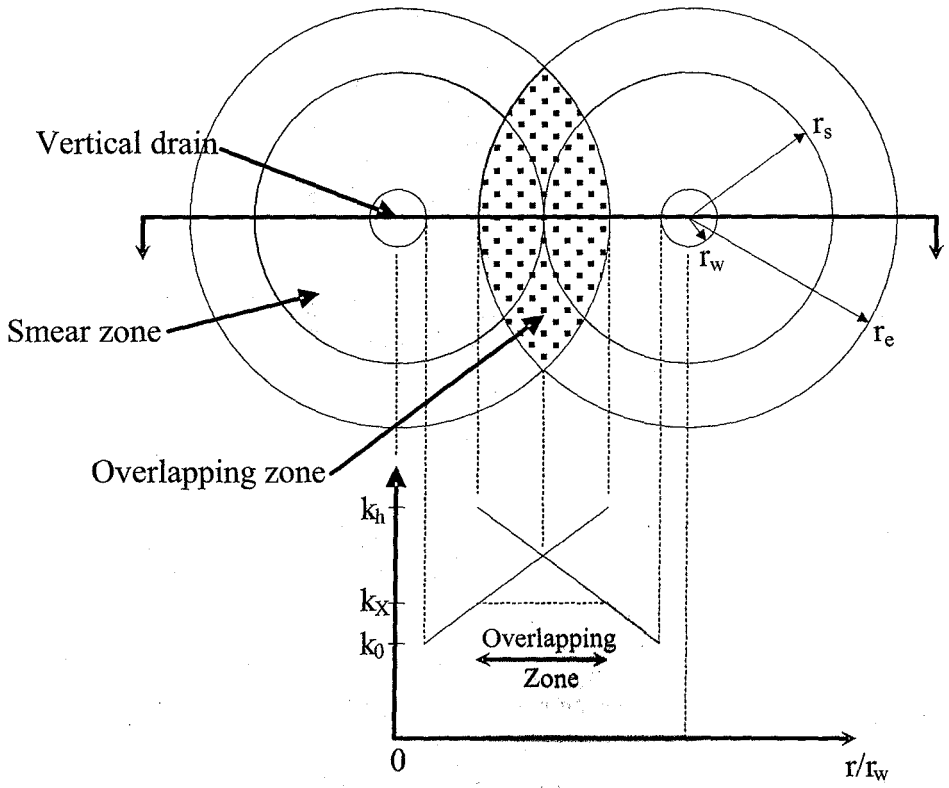

Figure 11: Schematic of overlapping smear zones (Walker and Indraratna, 2007).

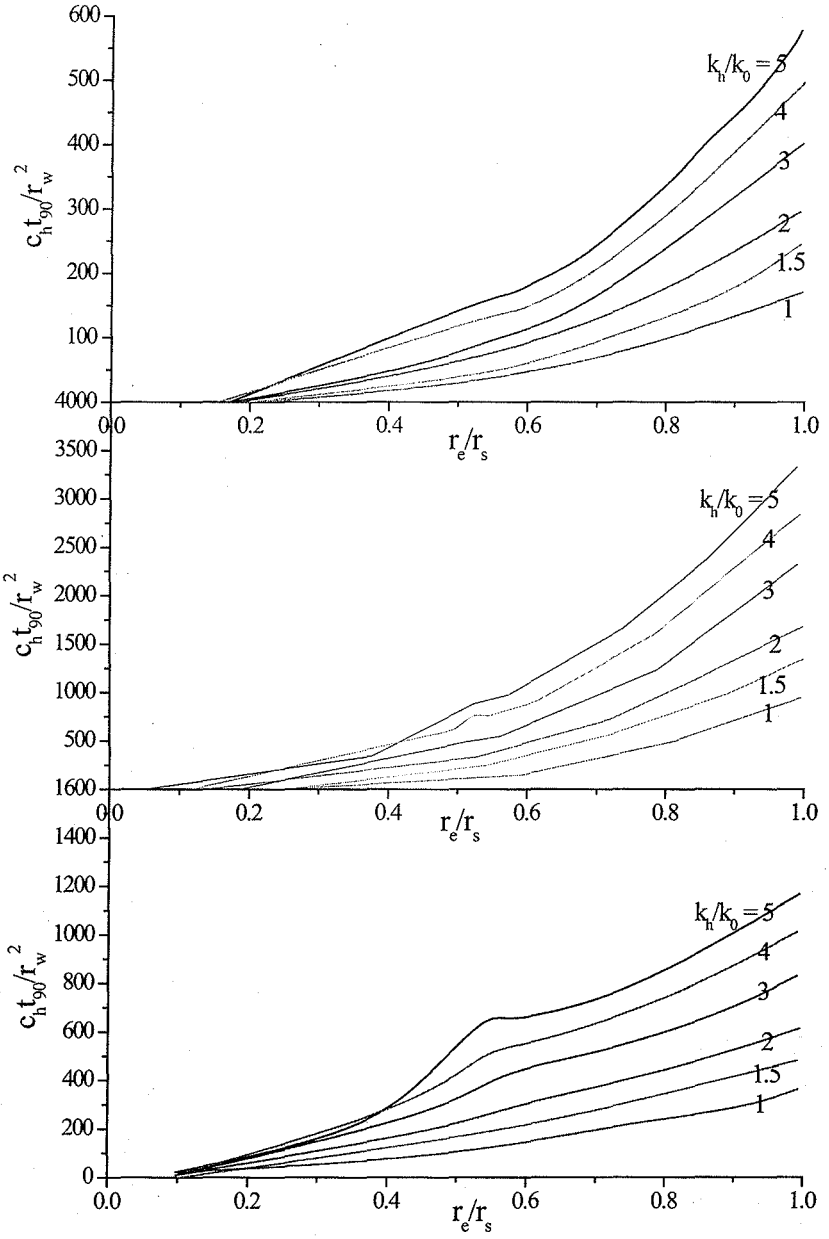

Figure 12: Time required for 90% consolidation for overlapping smear zones with linear variation of permeability: (a) $m_v / m_{v0} = 1$, $r_s / r_w = 10$; (b) $m_v / m_{v0} = 1$, $r_s / r_w = 20$; (c) $m_v / m_{v0} = 0.25$, $r_s / r_w = 10$ (Walker and Indraratna, 2007).

4.2 EFFECT OF REMOVING AND RE-APPLYING A VACUUM

A large-scale consolidometer can be utilised to examine the effect of vacuum preloading in conjunction with the surcharge load (Indraratna *et al.* 2004). A large scale consolidation test was conducted by applying a vacuum pressure close to the theoretical maximum of 100 kPa to the PVD and the soil surface through the centre hole in the rigid piston. A surcharge pressure was then applied in two stages, 50 kPa, and 100 kPa. The vacuum pressure was released for a short time in two stages over a 28 day period, to investigate the effect of unloading and reloading (Fig. 13a).

The laboratory results indicated that the suction head decreased with the depth of the drain because a maximum suction of 100 kPa could not be maintained along the entire length of the drain. The settlement associated with a combined vacuum and surcharge load is shown in Fig. 13b, which clearly reflects the effect of removing and re-applying the vacuum by the corresponding gradient settlement plot. The above experimental procedure also showed that it is very difficult to sustain a vacuum pressure greater than 90 kPa, (the theoretical maximum is 100 kPa)

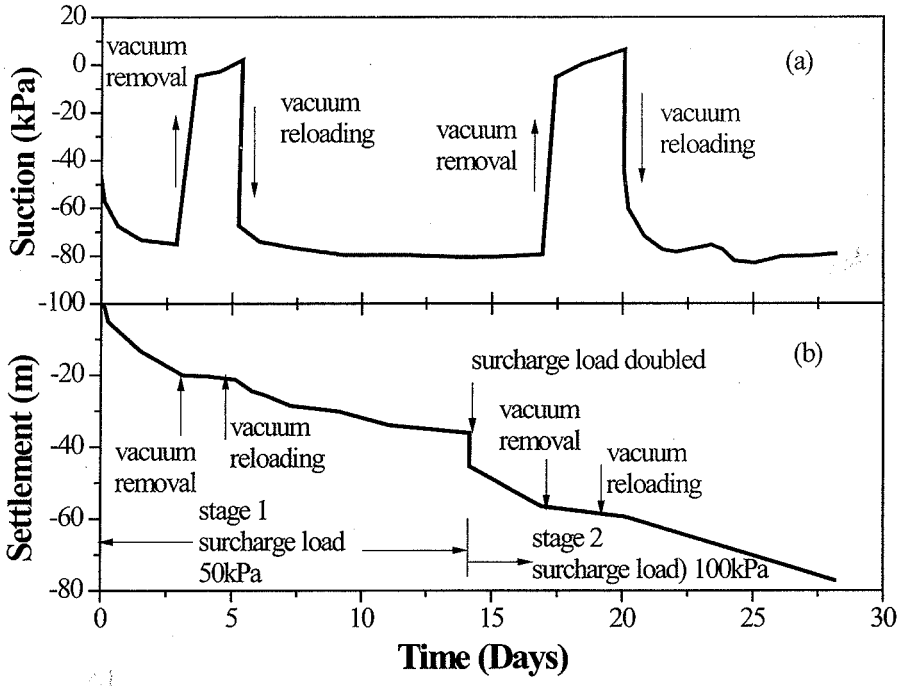

Figure 13: a) Suction in the drain (240 mm from bottom); b) surface settlement surface settlement associated with simulated vacuum loading and removal (Indraratna *et al.*, 2004).

4.3 SOIL DISTURBANCE DURING MANDREL INSTALLATION AND REMOVAL

When a mandrel is removed quickly, the soil near the drain can become unsaturated, i.e. an air gap. Indraratna *et al.* (2004) attempted to describe the apparent retardation of excess pore pressure dissipation using a series of models in large scale laboratory tests, whilst considering the effects of unsaturation at the drain-soil interface. The consolidation of soft clay in the large scale consolidometer under a combined vacuum and surcharge preloading was analysed using the FEM programme ABAQUS employing the modified Cam-clay theory (Roscoe and Burland, 1968). Figure 14 illustrates the plane strain finite element mesh using 8-noded linear strain quadrilateral elements (CPE8RP) with 8 displacement nodes and 4 pore pressure nodes. The associate shape functions for displacements and pore pressure are quadratic and linear respectively.

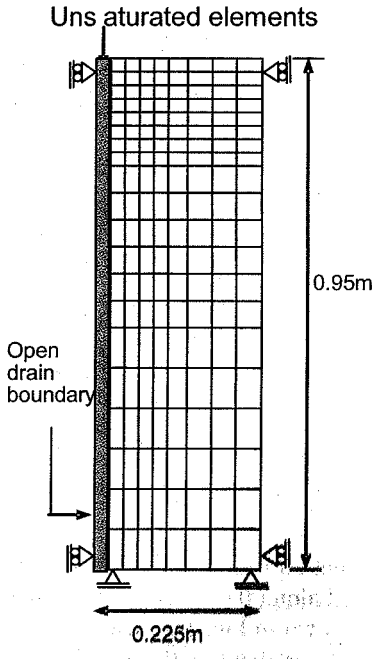

Figure 14: FEM discretization for plane strain analysis in large-scale consolidometer (Indraratna *et al.*, 2004).

The soil moisture characteristic curve (SMCC), including the effect of drain unsaturation could be captured by a thin layer of elements governed by elastic properties. The permeability coefficients converted to the 2D plane strain condition were based on the technique introduced by Indraratna and Redana (2000). Three distinct models were analysed, as summarised below:

Model 1 – fully saturated soil with a linear vacuum pressure distributed along the drain, (suction could be reduced to zero at the pressure bottom of drain).

Model 2 – The soil was fully saturated initially. When a linearly varying vacuum was applied, a layer of unsaturated elements was created at the PVD boundary. For convenience, the thin unsaturated layer was modelled elastically (E = 1000 kPa, ν=0.25).

Model 3 – Conditions were similar to Model 2, but included a time-dependent variation in the vacuum pressure (i.e. vacuum removal and reloading) to represent typical field conditions

Figure 15 shows the surface settlement predicted by the models described above. These predictions confirmed that the assumption of an unsaturated layer of soil at the drain-soil boundary with a time dependent variation in vacuum pressure (Model 3) was justified. Not surprisinsly, the condition of full saturation Model 1 over-predicted the settlement.

The predicted and measured values of excess pore water pressure (mid layer) are presented in Fig. 16. Clearly, the Models 2 and 3 are in acceptable agreement with the laboratory observations. As expected, Model 1 (fully saturated) gives the lowest pore pressure suggesting that the unsaturated soil-drain boundary certainly retards the dissipation of excess pore water pressure. In view of both settlement and excess pore water pressure, Model 3 provides the most accurate prediction compared to the laboratory data. Applying a vacuum head accelerates consolidation by increasing the lateral hydraulic gradient. Never the less, any soil unsaturation at the PVD boundary caused by mandrel driving would retard the excess pore pressure dissipation during the early stages of consolidation. To simulate how a mandrel disturbs the soil near the drain, Ghandeharioon *et al.* (2010) postulated that installing PVDs with a rectangular (conventional) steel mandrel would cause an elliptical cavity expansion with a concentric progression in the horizontal plane (Fig. 17).

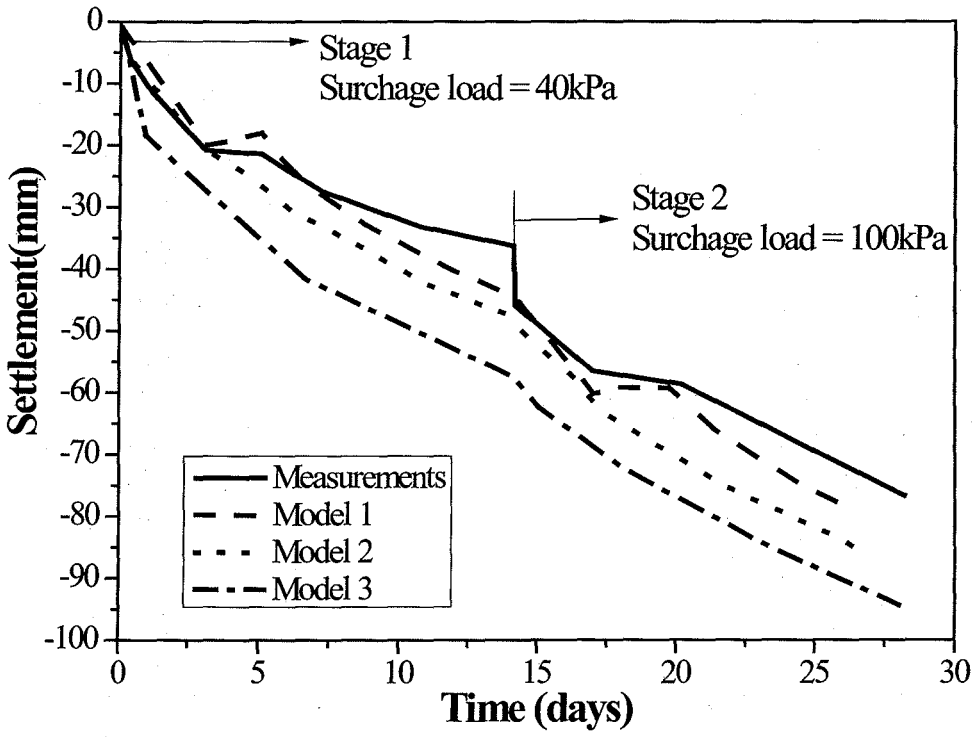

Figure 15: Predicted and measured settlement at the top of the consolidometer cell (Indraratna *et al.*, 2004).

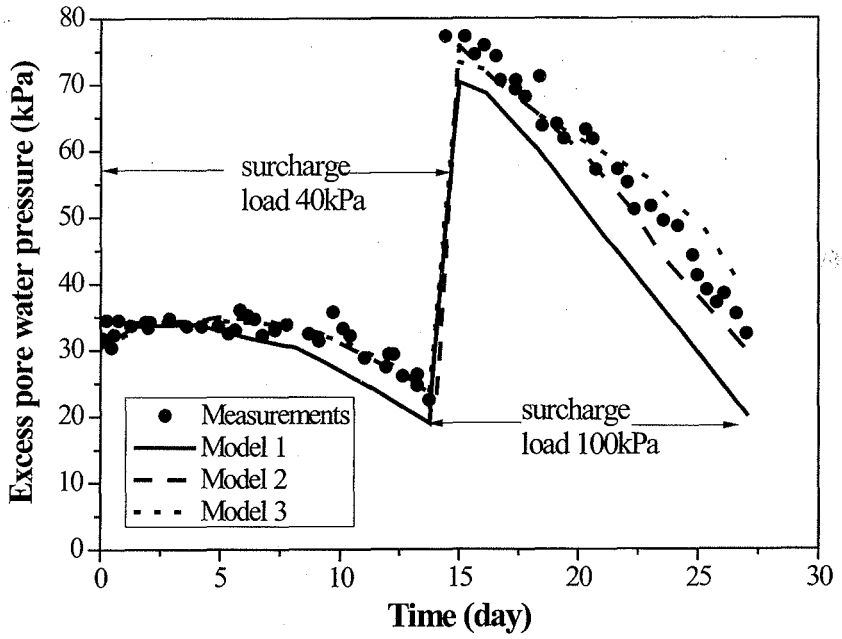

Figure 16: Predicted and measured pore-water pressure at transducer T2 (Indraratna *et al.*, 2004).

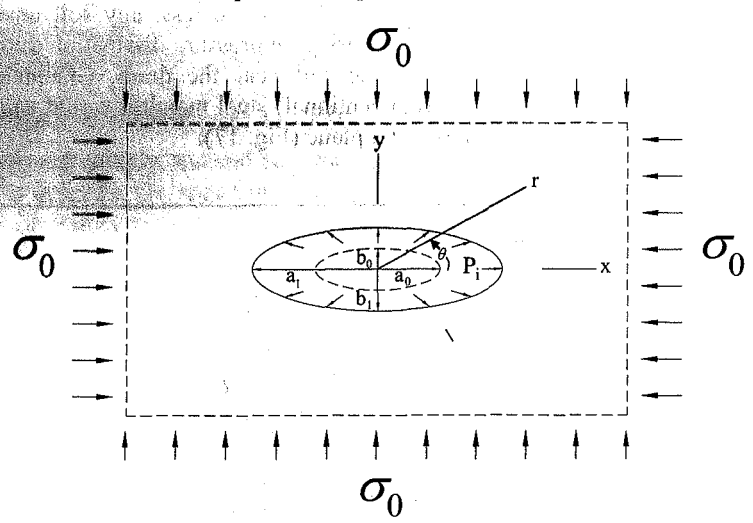

Figure 17: Expansion of an elliptical cavity in an infinite soft saturated cohesive soil, shown in polar coordinates (Ghandeharioon *et al.* 2010).

The elliptical cavity expansion theory (CET) was formulated using modified Cam-clay parameters to address the undrained analysis of PVDs installed in soft clay deposits. Mathematically, this process based on polar coordinates accounts for the rate of mandrel penetration and the time factor for predicting the internal pressure in the cavity, and the corresponding stresses and excess pore water pressure in the soil while driving the mandrel. The trend of excess pore pressure was verified by the laboratory results obtained from a fully instrumented large-scale consolidometer (Fig. 18).

An elliptical smear zone based on the CET was introduced while the disturbed soil surrounding the mandrel was characterised by plastic shear strain normalised by the rigidity index. As shown in Fig. 19, the analysis of three different cases mentioned above revealed that this term $\frac{\gamma_q^p q_f}{\sqrt{3}G}$ was 0.86% - 1.05% of the boundary of the failed soil. (γ_q^p was the plastic shear strain, $q_f = Mp_0'\left(\frac{n_p}{2}\right)^{\Lambda}$, M is the slope of critical state line in the p' and q plane; p_0' is the Initial effective mean stress, n_p is the isotropic over-consolidation ratio, Λ is the plastic

volumetric strain ratio, G is the shear modulus). The smear zone propagates outward where the normalised plastic shear strain within the smear zone was from 0.10%-0.17%, and at the boundary of the marginally disturbed zone, the magnitude of $\frac{\gamma_q^p q_f}{\sqrt{3}G}$ was about 0.01%-0.05% (Fig.19). The region where γ_q^p was greater than zero constituted the plastic zone, while the outer elastic zone (zero plastic shear strain) was not affected by any change in the excess pore water pressure before or after driving the mandrel. The dimensionless ratio of plastic shear strain to the rigidity index was useful for estimating the extent of the smear zone, because, it facilitated the use of basic soil parameters in purchase simulation without sophisticated large scale testing. The results also confirmed that the radius of the smear zone was at least 3 times the equivalent radius of the mandrel, a value close to the extent of smear zones suggested by previous studies. (Bergado *et al.*, 1991; Indraratna and Redana, 1997.)

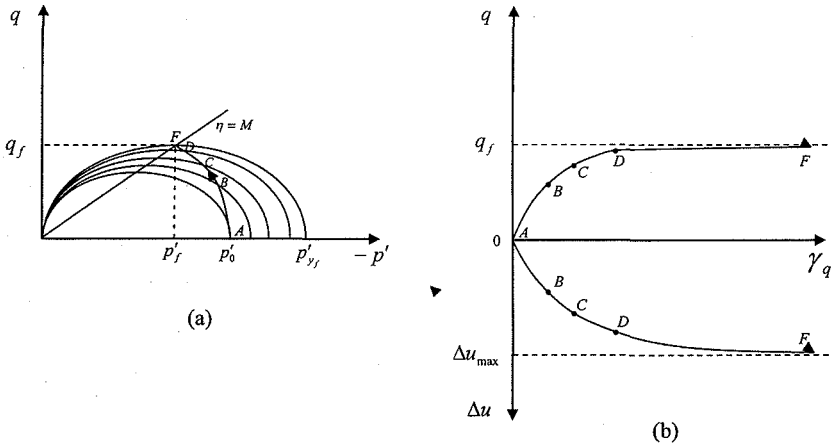

Figure 18: An undrained triaxial compression test on normally consolidated soil (a) effective stress path; and (b) deviator stress/excess pore pressure versus shear strain (Ghandeharioon *et al.*, 2010).

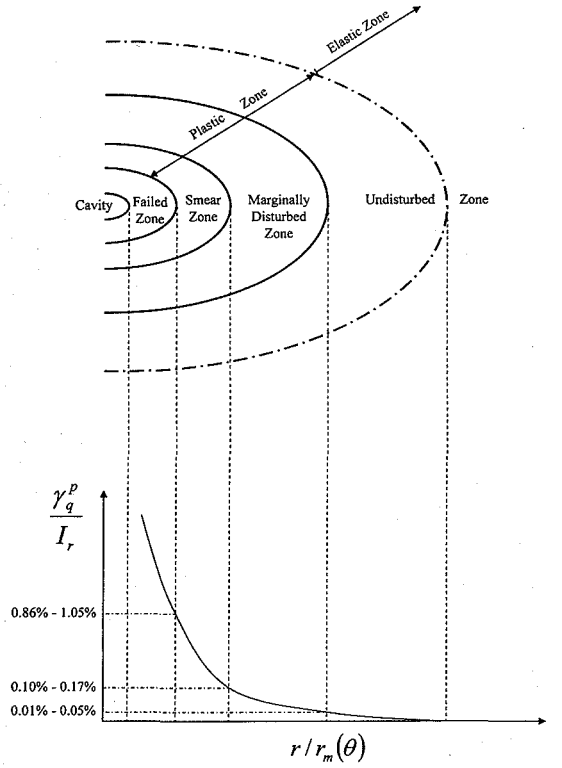

Figure 19: The distribution pattern for the ratio of the plastic shear strain to the rigidity index in relation to the radial distance normalized by the equivalent elliptical radius of the mandrel characterizing the disturbed soil surrounding a PVD (Ghandeharioon *et al.*, 2010).

4.4 THE EFFECT OF VACUUM CONSOLIDATION ON THE LATERAL YIELD OF SOFT CLAYS

In order to investigate the effect of a combined vacuum and surcharge load on lateral displacement, a simplified plane strain (2-D) finite element analysis could be used (Indraratna *et al.*, 2008). The outward lateral compressive strain due to surcharge can be reduced by applying suction (vacuum preloading). The optimisation of vacuum and surcharge preloading pressure to obtain a given settlement must be considered in any numerical model to minimise lateral displacement at the embankment toe (Fig. 20a), while identifying any tension zones where the vacuum pressure may be excessive.

As expected, the vacuum pressure alone can create inward lateral movement, whereas preloading without any vacuum may contribute to an unacceptable outward lateral movement. The particular situations for most clays is generally a combination of 40% surcharge preloading stress with a 60% vacuum, which seems to maintain a lateral displacement close to zero. Fig. 20b presents the various profiles of surface settlement with an increasing surcharge loading. A vacuum alone may generate settlement up to 10 m away from PVD treated boundary while the application of VP can minimise the value of soil heave beyond the embankment toe.

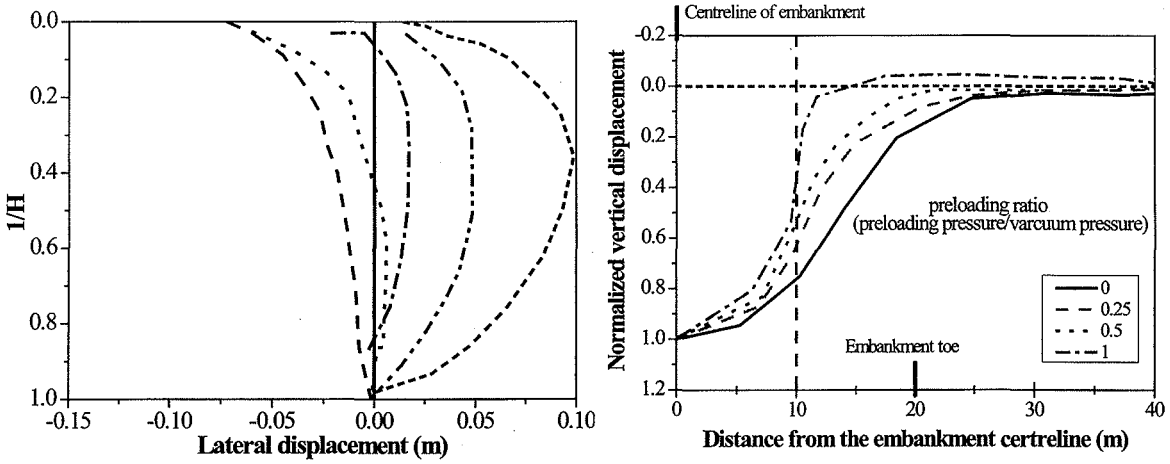

Figure 20: (a) Lateral displacements; and (b) surface settlement profiles (Indraratna *et al.*, 2008).

4.5 PARTIALLY PENETRATING DRAINS

In some situations, the soft clay is too deep for PVDs to penetrate fully, or the vertically propagated load will not be high enough to justify the full penetration of PVD into the entire clay layer. Therefore, consolidating the clay with partially penetrating vertical drains will be adequate. Indraratna *et al.* (2008) have numerically analysed the effects of partially penetrating vertical drains and vacuum pressure on the corresponding settlement and lateral displacement.

Figure 21 illustrates the effect of partially installed vertical drains (i.e. different l1/H ratios) on the overall degree of consolidation (Fig. 21a) and lateral displacement (Fig. 21b). The degree of consolidation was calculated on settlement at the centre line and lateral displacement at the embankment toe. The drain may be reduced in length by up to 90% of the entire thickness of clay without significantly affecting the degree of consolidation. The lateral displacements are rather insensitive to the PVD level, as shown in Fig. 21b. As shown in Fig. 22a, vertical drains are assumed to be installed to a depth l_2, while the drains in between these are installed to the entire depth of clay (H). It can be seen that l_2 can be reduced by up to $0.6H$ without any significant increase in the time for 90% primary consolidation to occur. In Fig. 22a, the primary PVD can be shortened by up to 80-90% of the thickness of the soil without seriously affecting the time for a given degree of consolidation, whereas alternating shorter drains can be reduced in length by up to 40% of the entire clay thickness.

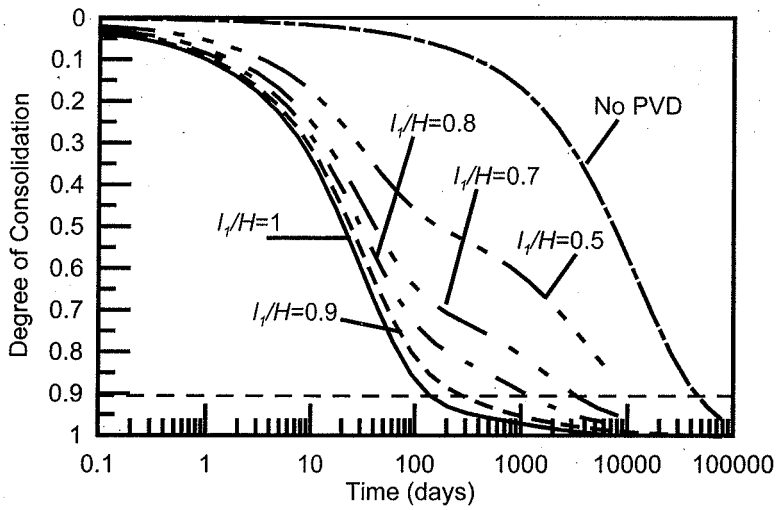

(a)

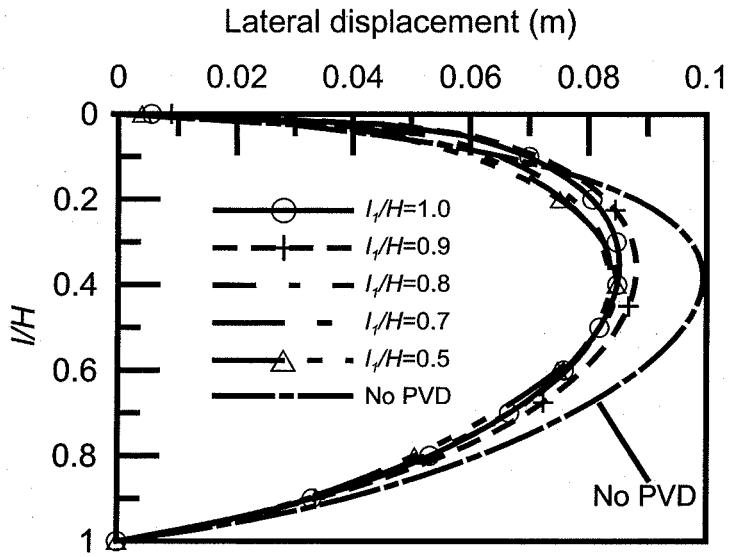

(b)

Figure 21: Effects on partially penetrating drains (equal length) on: (a) degrees of consolidation; and (b) lateral displacement (Indraratna *et al.*, 2008).

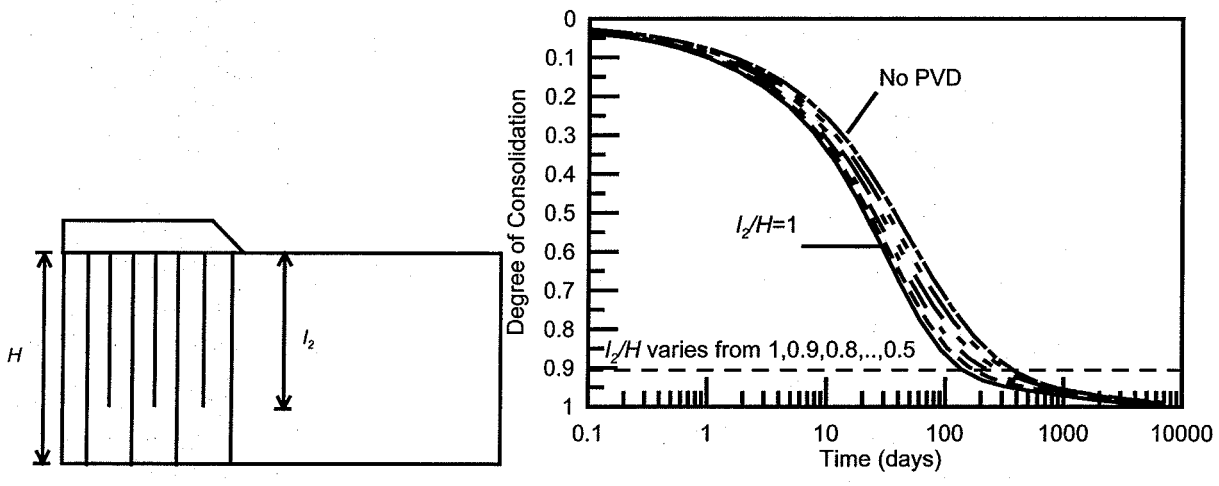

(a) (b)

Figure 22: (a) Vertical drains with alternating length; and (b) effects on the degree of consolidation (Indraratna *et al.*, 2008).

4.6 NON-DARCIAN FLOW

Hansbo (1997) stated that at small hydraulic gradients, conventional (linear) Darcy's law may be replaced by a non-Darcian flow condition defined by an exponential relationship. Based on non-Darcian flow, Hansbo (1997) modified the classical axi-symmetric solutions. The pore water flow velocity v, caused by a hydraulic gradient i, might deviate from the original Darcy's law $v = k\ i$, where under a certain gradient i_o below which no flow occurs. Then the rate of flow is given by $v = k\ (i - i_o)$, hence the following mathematical relations have been proposed:

$$v = \kappa i^n \ for \ i \le i_1 \tag{7}$$

$$v = k(i - i_o) for \ i \ge i_1 \tag{8}$$

where

$$i_1 = \frac{i_o n}{(n-1)} \text{ and } \kappa = \left(n^{-1} i^{1-n}\right) k \tag{9}$$

In order to study the effects of non-Darcian flow, Hansbo (1979, 1997) proposed an alternative consolidation equation. The time required to reach a certain average degree of consolidation including smear effect is given by:

$$t = \frac{\alpha D^2}{\lambda}\left(\frac{D\gamma_w}{u_o}\right)^{n-1}\left(\frac{1}{\left(1-\bar{U}_h\right)^{n-1}} - 1\right) \tag{10}$$

where the coefficient of consolidation $\lambda = \frac{\kappa_h M}{\gamma_w}$, $M=1/m_v$ is the oedometer modulus, D is the diameter of the drain influence zone, d_s is the diameter of smear zone, $n=D/d_w$ in which d_w is the drain diameter, u_o is the initial average excess pore water pressure, and α is determined explicity as a high non-linear function of n, D/d and κ_h / κ_s. (Hansbo 1997).

When $n \to 1$ Eq. **(10)** gives the same result as the average degree of consolidation represented as $T_h = c_h t / d_e^2$, provided the well resistance is neglected.

Sathananthan *et al.* (2006b) developed a new plane strain lateral consolidation equation, which can be applied to the exponential and linear correlation between the hydraulic gradient and flow velocity, while neglecting the well resistance of vertical drains. A comparison was made between the results obtained by a Darcian (linear) flow solution and the new solution based on a non-Darcian (exponential) flow.

The parameters described by Sathananthan and Indraratna (2006b) under plane strain condition are:

$$\bar{U}_{hp} = 1 - \left[1 + \frac{\lambda_{hp} t}{\alpha_p (2B)^2}\left(\frac{\bar{u}_0}{B\gamma_w}\right)^{n-1}\right]^{\frac{1}{1-n}} \tag{11}$$

where subscript p stands for plane strain; $\lambda_{hp} = \kappa_{hp} / m_v \gamma_w$, B is the half width of plane strain unit cell (m); $\bar{u}_0$ is the initial average excess pore water pressure (kN/m^2); and

$$\alpha_p = \frac{\beta_p^n}{4(n-1)} \tag{12a}$$

$$\beta_p = \left(\frac{\kappa_{hp}}{\kappa_{sp}}\right)^{\frac{1}{n}}\left[f_p\left(n, \frac{b_w}{B}\right) - f_p\left(n, \frac{b_s}{B}\right)\right] + f_p\left(n, \frac{b_s}{B}\right) \tag{12b}$$

$$f_p(n,y)=\left[\frac{1}{2!}-\frac{1}{3!n}-\frac{(n-1)}{4!n^2}-\frac{(n-1)(2n-1)}{5!n^3}-\frac{(n-1)(2n-1)(3n-1)}{6!n^4}-.....\right]$$

$$-y-\frac{(n-1)}{2!n}y^2+\frac{(2n-1)}{3!n^2}y^3+\frac{(n-1)(3n-1)}{4!n^3}y^4 \qquad \textbf{(12c)}$$

$$+\frac{(n-1)(2n-1)(4n-1)}{5!n^4}y^5+\frac{(n-1)(2n-1)(3n-1)(5n-1)}{6!n^5}y^6+.....$$

It is noted that $k_{hp}/k_h=\lambda_{hp}/\lambda$, because, the coefficient of permeability is proportional to the coefficient of consolidation for a particular soil of given compressibility. Figure 23 shows the variation in the equivalent parameters (α_p, β_p, $k_{hp}/k_h=\lambda_{hp}/\lambda$, and k_{hp}/k_{sp}) with spacing ratio (B/b_w), smear ratio (b_s/b_w), and permeability ratio (k_h/k_s) of the axi-symmetric cell for n = 1.5. Figure 24 shows a comparison between Darcian and non-Darcian analysis. The field data agree with the non-Darcian analysis.

The advantage of the above equivalent plane strain procedure is that it not only matches the average degree of radial consolidation (axi-symmetric), but it also yields a more realistic distribution of excess pore pressure in the lateral direction compared to the Darcian condition. It was verified that the conventional solution based on conventional Darcian flow ($v = ki$) was better when it was replaced with an exponential equation ($v=\kappa n i_1^{n-1}$). It was also demonstrated that for $n\rightarrow 1$, the current non-Darcian solution approached the Darcian solution proposed earlier by Indraratna and Redana (1997), with a deviation of less than 0.01%. This analysis showed that the consolidation process was clearly influenced by the exponent factor n. The graphical representations of equivalent plane strain parameters as a function of the spacing ratio, smear ratio and the permeability ratio of the axi-symmetric cell (e.g. Fig. 23), would facilitate the practical use of this theory.

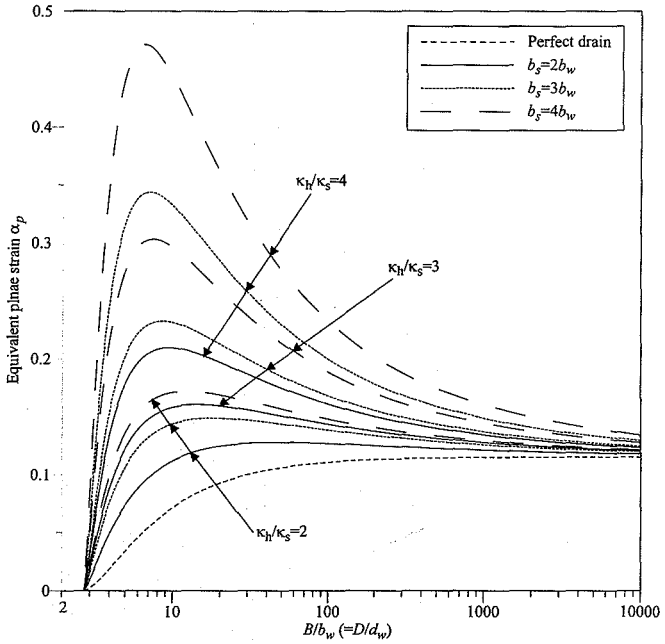

Figure 23: Equivalent plane strain α_p value as a function of B/b_w, b_s/b_w and κ_h/κ_s of axi-symmetric unit cell for n=1.5 (Sathananthan *et al.*, 2006b).

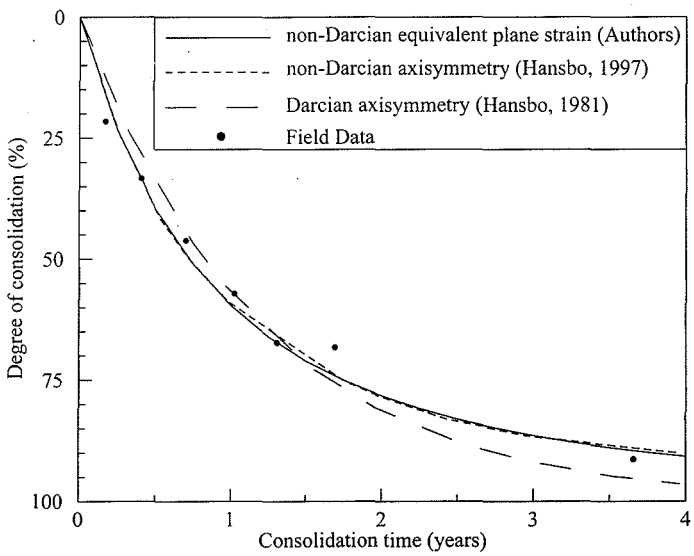

Figure 24: Variation of degree of consolidation at the embankment centreline with time for the test Area II at Ska-Edeby, Sweden field test (Sathananthan *et al.*, 2006b).

4.7 PERFORMANCE OF PVD SUBJECTED TO CYCLIC LOADING

Low lying areas with high volumes of plastic clays can sustain high excess pore water pressure during static and repeated cyclic loading. The effectiveness of prefabricated vertical drains (PVD) for dissipating cyclic pore water pressures has been discussed by Indraratna *et al.* (2009a).

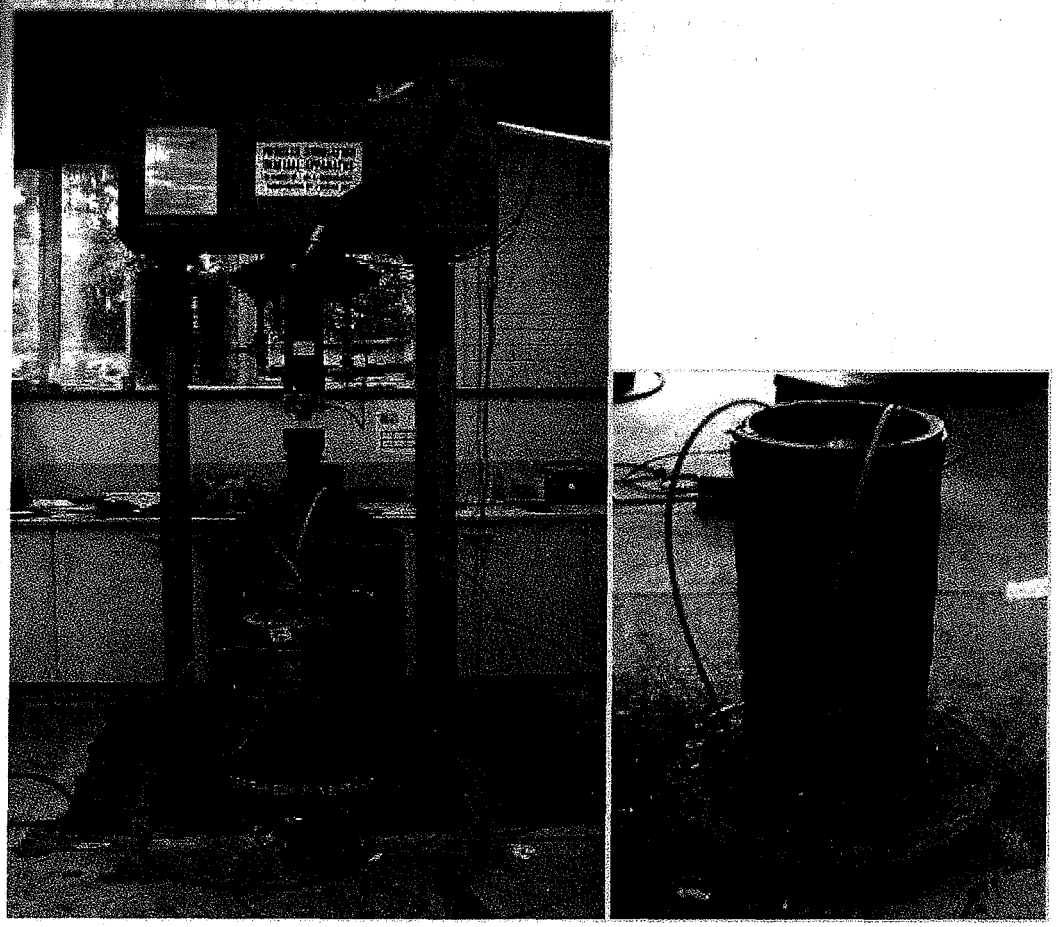

Figure 25: (a) Large-scale triaxial rig; (b) soil specimen (Indraratna *et al.*, 2009a).

A large scale tri-axial test was used to examine the effects of cyclic load on radial drainage and consolidation by PVDs (Fig. 25a). This test chamber can accommodate specimens 300 mm diameter and 600 mm high (Fig. 25b). The excess pore water pressure was monitored via miniature pore pressure transducers. These instruments were

saturated under distilled water with vacuum pressure, and then fitted through the base of the cell to the desired locations on the samples.

The test specimen of reconstituted estuarine clay was lightly compacted to a unit weight of about 17 to 17.5 kN/m^3. Ideally, testing requires the simulation of k_0 conditions that may typically vary in many coastal regions of Australia from 0.6-0.7. Most soft clays will have natural water contents that exceed 75% and a Plasticity Index > 35%. It is not uncommon to find that the undrained shear strengths of the soft estuarine deposits are less than 10 kPa. In Northern Queensland, some very soft clays that have caused embankment problems have been characterised by c_u values < 5 kPa.

The tests could be conducted at frequencies of 5-10 Hz, typically simulating train speeds of say 60-100 km/h with 25-30 tonnes/axle train loads. Figure 26 shows an example of the excess pore pressure recorded This indicates that the maximum excess pore water pressure beside the PVD during cyclic load (T4) were significantly less than that near the cell boundary (T3). And as expected, the excess pore pressure close to the boundary of the outer cell (e.g. T1 and T3) dissipated at a slower rate than the transducers T4 and T2, which were closer to the PVD than T1.

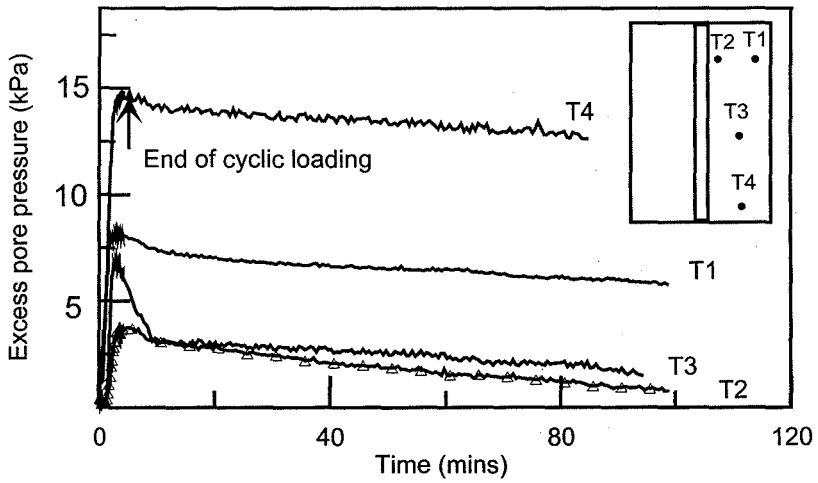

Figure 26: Dissipation of excess pore pressure at various locations from the PVD (Indraratna *et al.*, 2009a).

Figure 27 shows the excess pore pressures and corresponding excess pore water pressure ratio R_u versus the number of loading cycles N under the three separate series of tests. Without PVD, the excess pore pressure increased rapidly R_u ⏲ 0.9, and undrained failure occurred very quickly. The corresponding axial strains are shown in Fig. 28a. Without a PVD, large cyclic axial strains developed and failure occurred rapidly after about 200 cycles in the cyclic CK_0U test, and after about 100 cycles in the cyclic UC (cyclic confined compression) test. As seen from Fig. 28b, failure was detected when $\varepsilon_a - \log N$ curves began to concave rapidly downwards. With a PVD, the axial strain gradually increased to a constant level and no failure was evident even after 3,000 cycles, as shown in Figs 28(a and b).

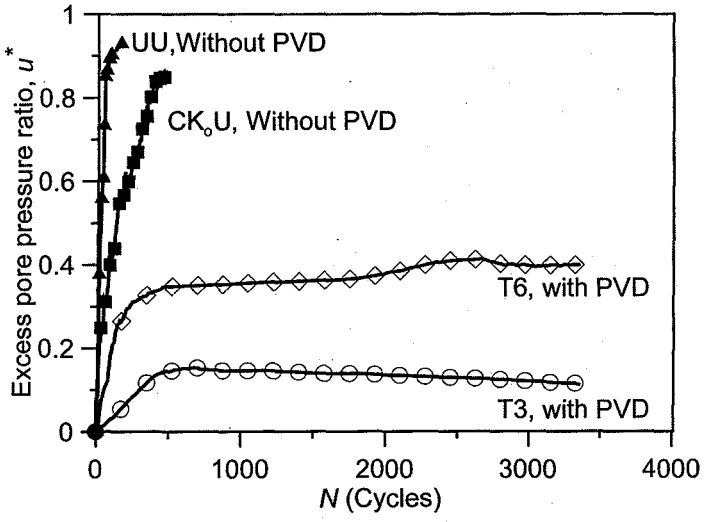

Figure 27: Excess pore pressure generated with and without PVD under cyclic loading (Indraratna *et al.*, 2009a).

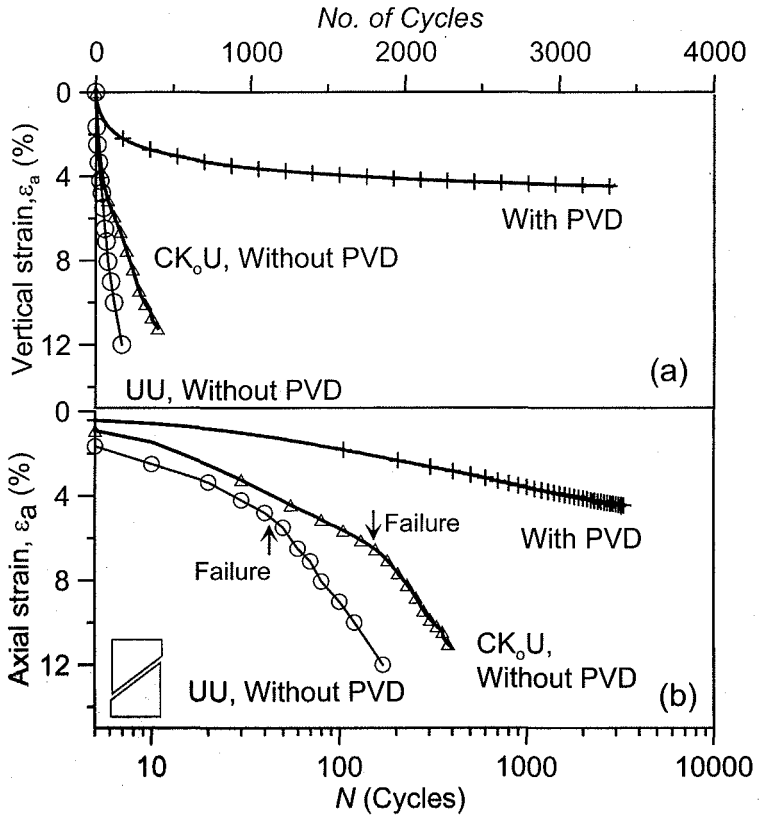

Figure 28: Axial strains during cyclic loading with and without PVD versus number of loading cycles (N): (a) arithmetic; (b) semi logarithmic scales (Indraratna *et al.*, 2009a).

The test results revealed that PVDs effectively decreased the maximum excess pore pressure, even under cyclic loading, and they also decreased the build up of excess pore pressure and helped to accelerate its dissipation during any rest periods. In reality, dissipating pore water pressure during a rest period stabilises the track for the next loading stage (i. e., subsequent passage of train). This cyclic-induced excess pore pressure tends to rise substantially as the shear strain exceeds 1.5-2%. Soft clays provided with radial drainage via PVD can be subjected to cyclic stress levels higher than the critical cyclic stress ratio without causing undrained failure.

In practice, railway tracks and airport runways are constantly subjected to relatively high cyclic loads that build up pore water pressures in the underlying subsoils unless sufficient drainage is provided. Laboratory experiments indicate that cyclic pore pressures build up rapidly at high frequencies and the rate of pore pressure dissipation is less than its rate of build up under cyclic loading. The Author worked as a consultant in the monitoring of the Sandgate rail track near Newcastle where relatively short drains were installed to stabilise the track that was constructed on at least 30m of soft estuarine clays in some areas of the track (Indraratna *et al.* 2010). As the vertical load from 25 tonne axle trains is mainly taken by the shallow subgrade, relatively short PVD were adequate to dissipate the cyclic excess pore water pressure (Fig. 29). Moreover, the short PVD also contributed to the control of laterals displacements on the shallow soft estuarine clay having effectively consolidated the very soft clay beneath the track within a period of a few months upon the initial passage of trains. In this case, no external surcharge fill was used as preloading and no vacuum application was required as only the shallow clay layer immediately beneath the ballast and subballast warranted stabilisation. A FEM model based on PLAXIS was used to simulate the track behaviour, and the Class A prediction of excess pore pressure, settlement and lateral movement was in very good agreement with the field data (Figs. 30 and 31). The field measurements were only made available to the Author one year after the FEM results had been submitted to the client.

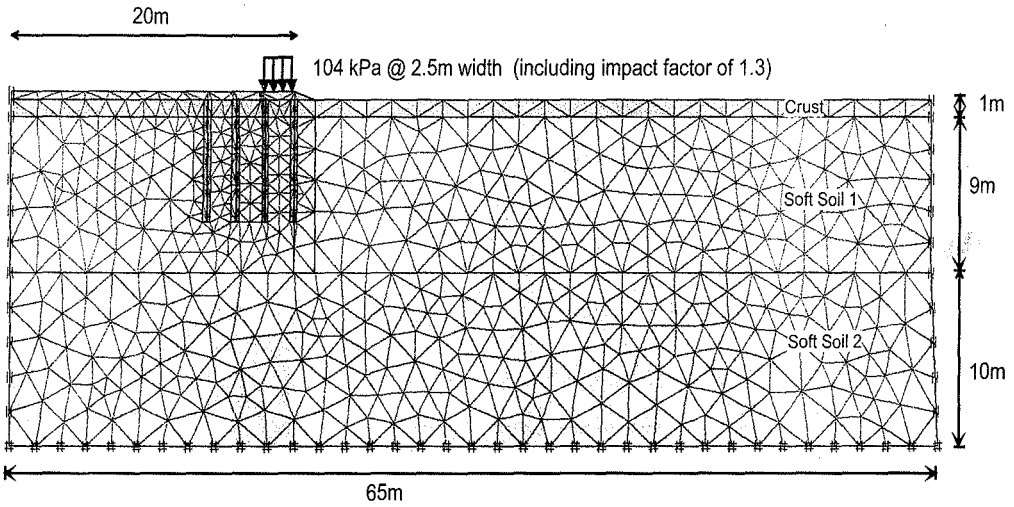

Figure 29: Vertical cross section of rail track and foundation (Indraratna *et al.*, 2010).

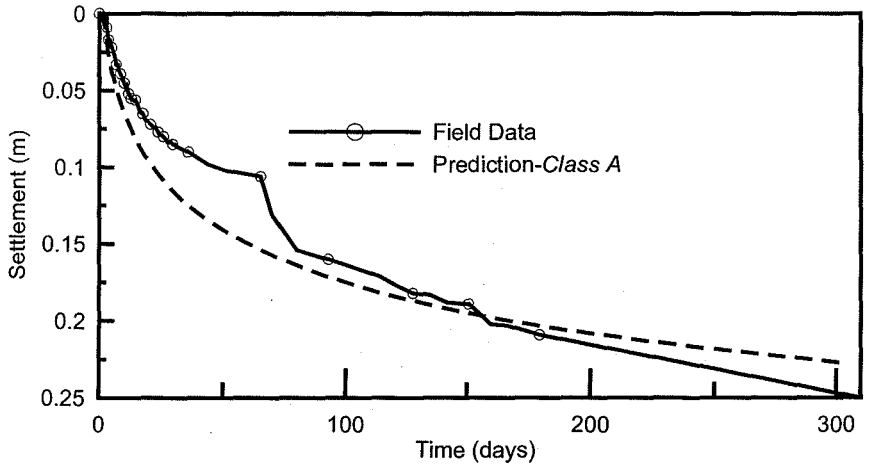

Figure 30: Predicted and measured settlement at the centre line of rail tracks (Indraratna *et al.*, 2010).

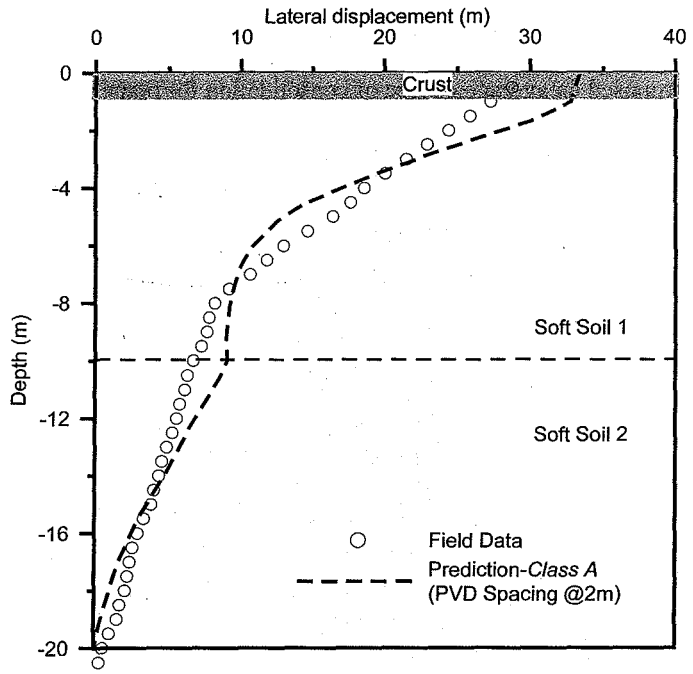

Figure 31: Measured and predicted lateral displacement profiles near the rail embankment toe after 180 days (Indraratna *et al.*, 2010).

5 NUMERICAL ANALYSIS

For multi-drain simulation, plane strain finite element analysis can be readily adapted to most field situations (Indraratna and Redana 2000; Indraratna *et al.* 2005a). Nevertheless, realistic field predictions require that the axi-symmetric properties to be converted to an *equivalent* 2D plane strain condition, especially the permeability coefficients and drain geometry. Plane strain analysis can also accommodate vacuum preloading in conjunction with vertical drains (e.g. Gabr and Szabo, 1997); Indraratna *et al.* (2005b) proposed an equivalent plane strain approach to simulate vacuum pressure for a vertical drain system with modification to the original theory introduced by Indraratna and Redana (1997), as shown in Fig. 29.

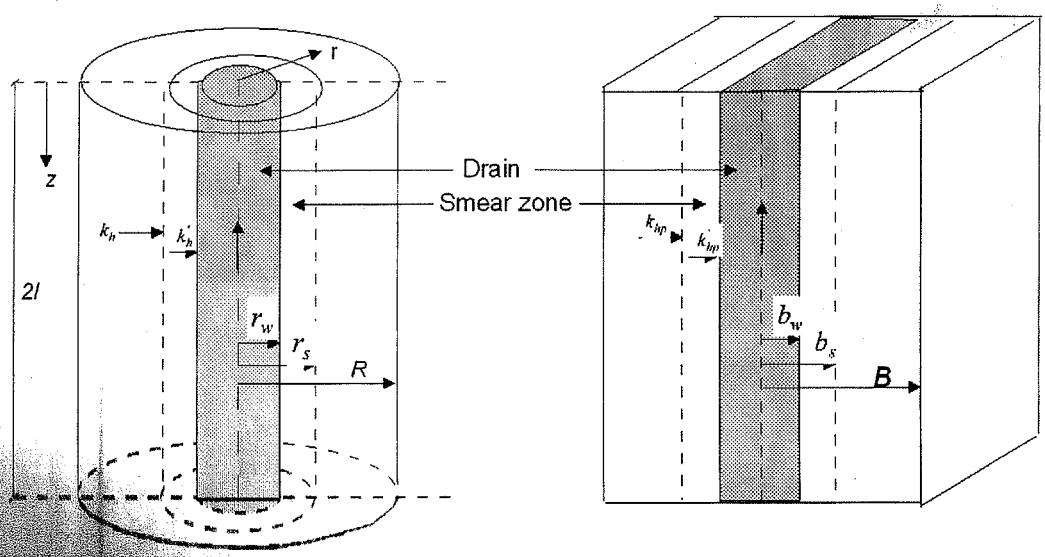

(a) Axi-symmetric (b) Plane strain

Figure 32: Conversion of an axisymmetric unit cell into plane strain condition (Indraratna *et al.*, 2005b).

Equivalent plane strain conditions can be fulfilled in three ways:

(1) Geometric approach where the PVD spacing varies, but the soil permeability remains constant;

(2) Permeability approach where the equivalent permeability coefficient is determined while the drain spacing remains unchanged;

(3) Combined permeability and geometric approach where plane strain permeability is calculated based on a convenient space between the drains.

Indraratna *et al.* (2005b) proposed an average degree of consolidation for plane strain by assuming that the plane strain cell (width of 2*B*), the half width of the drain b_w and the half width of the smear zone b_s may be kept the same as their axi-symmetric radii r_w and r_s, respectively. This implies that $b_w = r_w$ and $b_s = r_s$ (Fig.32). To excess pore pressure can be determined form:

$$\frac{\bar{u}}{\bar{u}_0} = \left(1 + \frac{p_{0p}}{\bar{u}_o}\frac{(1+k_1)}{2}\right)\exp\left(-\frac{8T_{hp}}{\mu_p}\right) - \frac{p_{0p}}{\bar{u}_0}\frac{(1+k_1)}{2} \qquad \textbf{(13a)}$$

and

$$\mu_p = \left[\alpha + (\beta)\frac{k_{hp}}{k'_{hp}}\right] \qquad \textbf{(13b)}$$

where $\bar{u}_0$ = the initial excess pore pressure, $\bar{u}$ = the pore pressure at time t (average values) and T_{hp} = the time factor in plane strain, and k_{hp} and k'_{hp} are the equivalent undisturbed horizontal and corresponding smear zone permeability, respectively. The geometric parameters α and β are given by:

$$\alpha = \frac{2}{3} - \frac{2b_s}{B}\left(1 - \frac{b_s}{B} + \frac{b_s^2}{3B^2}\right) \qquad \textbf{(14a)}$$

$$\beta = \frac{1}{B^2}(b_s - b_w)^2 + \frac{b_s}{3B^3}\left(3b_w^2 - b_s^2\right) \qquad \textbf{(14b)}$$

At a given level of effective stress, and at each time step, the average degree of consolidation for the axi-symmetric ($\overline{U}_p$) and equivalent plane strain ($\overline{U}p, pl$) conditions are made equal.

By making the magnitudes of R and B the same, Indraratna *et al.* (2005a) presented a relationship between k_{hp} and k'_{hp}. The smear effect can be captured by the ratio between the smear zone permeability and the undisturbed permeability, hence:

$$\frac{k'_{hp}}{k_{hp}} = \frac{\beta}{\frac{k_{hp}}{k_h}\left[\ln\left(\frac{n}{s}\right) + \left(\frac{k_h}{k'_h}\right)\ln(s) - 0.75\right] - \alpha} \tag{15}$$

Ignoring the effects of smear and well resistance in the above expression would lead to the simplified solution proposed earlier by Hird *et al.* (1992):

$$\frac{k_{hp}}{k_h} = \frac{0.67}{[\ln(n) - 0.75]} \tag{16}$$

Indraratna *et al.* (2005b) compared two different distributions of vacuum along a single drain for the equivalent plane strain (2D) and axi-symmetric conditions (3D). Varying the vacuum pressure in prefabricated vertical drains installed in soft clay would be more realistic for long drains, but a constant vacuum with depth is justified for relatively short drains

6 CASE HISTORIES

6.1 PORT OF BRISBANE

The Port of Brisbane is located at the mouth of the Brisbane River at Fisherman Islands. An expansion of the Port includes a 235ha area to be progressively reclaimed and developed over the next 20 years, using dredged materials from the Brisbane River and Moreton Bay shipping channels. The site contains compressible clays of over 30 m in thickness. At least 7 m of dredged mud capped with 2 m of sand was used to reclaim the sub-tidal area. Generally, the complete consolidation of the soft deep clay deposits may well take in excess of 50 years, if surcharging was the only treatment, with associated settlements of probably 2.5 - 4 m likely. To reduce the consolidation period, the method of prefabricated vertical drains (PVD) and surcharge or PVD combined with vacuum pressure (at sites where stability is of a concern) were chosen to be trialled. Three contractors undertook the trial works being Austress Menard, Van Oord and Cofra/Boskalis. All three trialed prefabricated drains and surcharge with Austress Menard and Cofra/Boskalis also trialing their respective proprietary membrane and membraneless vacuum systems. Figure 33 shows the final layout of a typical trial area with the PVD design results for each area.

The typical soil properties are summarised in Table 1.

Table 1 Typical Soil Properties (Port of Brisbane Corporation and Austress Menard, 2008).

Soil layer	Soil type	g_t (kN/m^3)	$Cc/(1+e_0)$	C_v (m^2/yr)	C_h (m^2/yr)	k_h/k_s	$s=d_s/d_w$	$Ca/(1+e_0)$
1	Dredged Mud	14	0.3	1	1	1	1	0.005
2	Upper Holocene Sand	19	0.01	5	5	1	1	0.001
3	Upper Holocene Clay	16	0.18	1	2	2	3	0.008
4	Lower Holocene Clay	16	0.235	0.8	1.9	2	3	0.0076

To compare two locations with a different loading history, the lateral displacement normalised by the applied effective stress at two inclinometer positions (MS24 and MS34) are plotted in Fig. 34. It was clear that the lateral displacements were largest in the upper Holocene shallow clay depths and were insignificant below 10m. From this limited inclinometer data, the membraneless BeauDrain system (MS34) had controlled the lateral displacement more effectively than the surcharge only section (MS24). Settlement and excess pore water pressure predictions and field data for a typical settlement plate (TSP3) are shown in Fig. 35. The predicated settlement curve agreed with the field data. The excess pore water pressures were more difficult to predict than settlement, but they did indicate a slower rate of dissipation in the Holocene clays in every section monitored, in spite of the PVDs. From the perspective of stability, the incremental rate of change of the lateral displacement/settlement ratio (μ) with time can be plotted as shown in Fig. 36. This rate of change of μ can be determined for relatively small time increments where a small and decreasing gradient can be considered to be stable with respect to lateral movement, while acontinuously increasing gradient of μ reflects potential lateral

instability. In Fig. 36, the gradient in the non-vacuum area WD3 increased initially, which could be attributed to the final surcharge loading placed quickly, while the clay was still at early stages of consolidation. However, as the PVDs become fully active and settlement increased at a healthy rate, the gradient of μ decreased, as expected. In general, Figure 36 illustrates that the vacuum pressure provides a relatively unchanging gradient of μ with time.

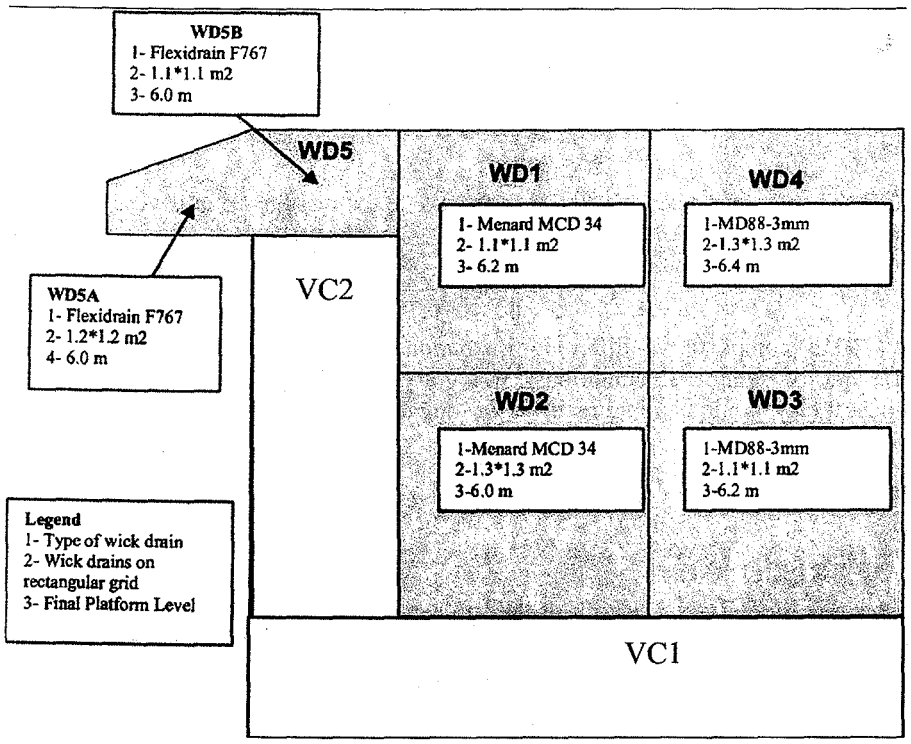

Figure 33: S3A Trial Area – Layout and detail design specifications (Port of Brisbane Corporation and Austress Menard, 2008).

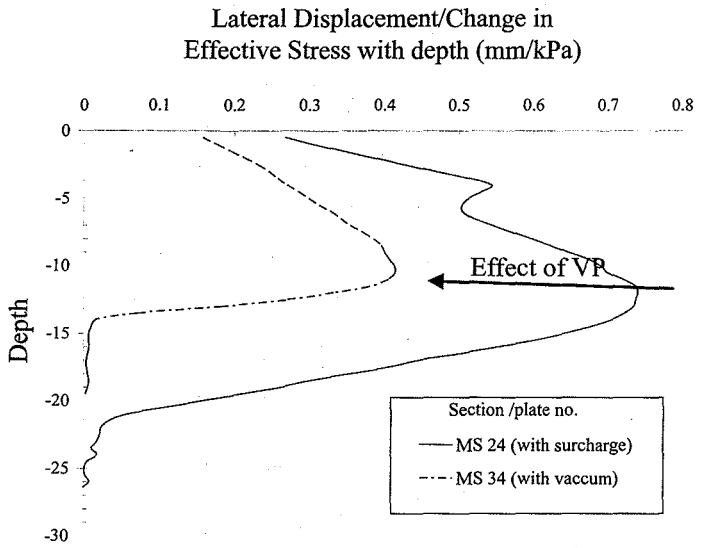

Figure 34: Comparison of lateral displacements in vacuum and non-vacuum areas.

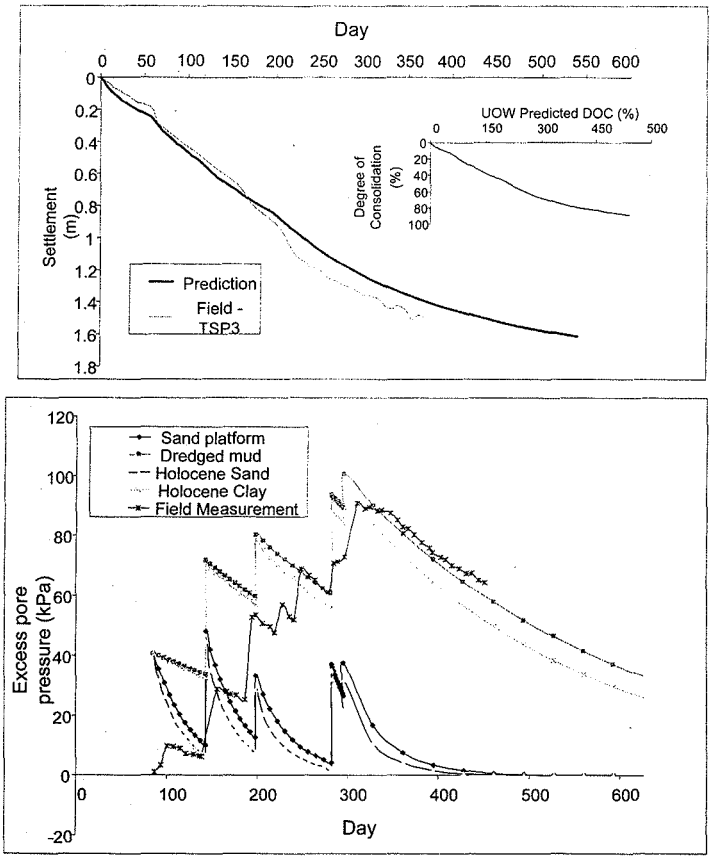

Figure 35: (a) Settlement; and (b) excess pore water pressure predictions and field data for a typical settlement plate location.

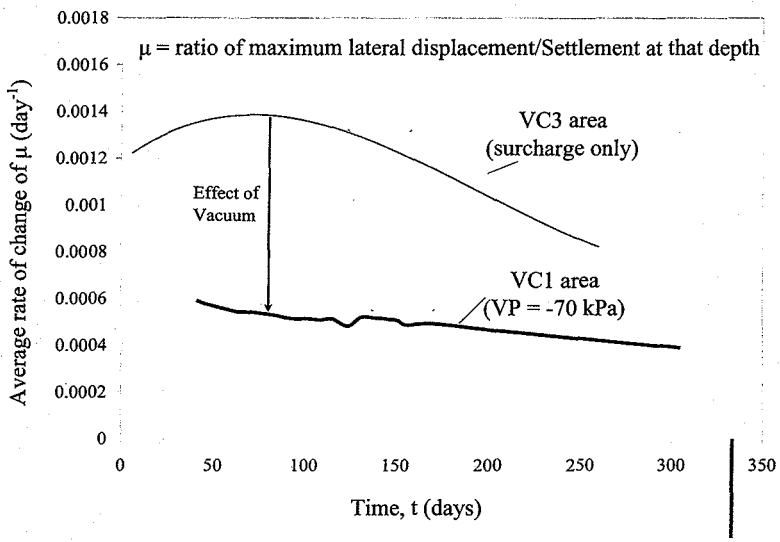

Figure 36: Rate of change of lateral displacement/settlement ratio with time.

Figure 37 provides approximately linear relationships between the long term residual settlement (RS) and the clay thickness of clay for an over-consolidation ratio (OCR) from 1.1 to 1.4, and for a degree of consolidation (DOC) that exceeding 80%. The reduced settlement (RS) was determined based on the theory secondary consolidation employing the secondary compression index C_α (Table 1). More detail on the computation of RS are given by Mesri and Castro (1987), Bjerrum (1972) and Yin and Clark (1994). As expected, when the OCR increased, the RS decreased substantially. In general, as the thickness of holocene clay increased, the RS also increased. The corresponding regression lines and best–fit equations are also shown in Figure 37. In particular, the vacuum consolidation locations (VC1-2, VC2-2 and VC2-3) show a considerably reduced RS at an OCR

approaching 1.4, which is well below the permissible limit of 250mm. At an OCR of approximately 1.3, the residual settlement associated with membraneless BeauDrain consolidation (TA8) and membrane type (VC1-5) were also small.

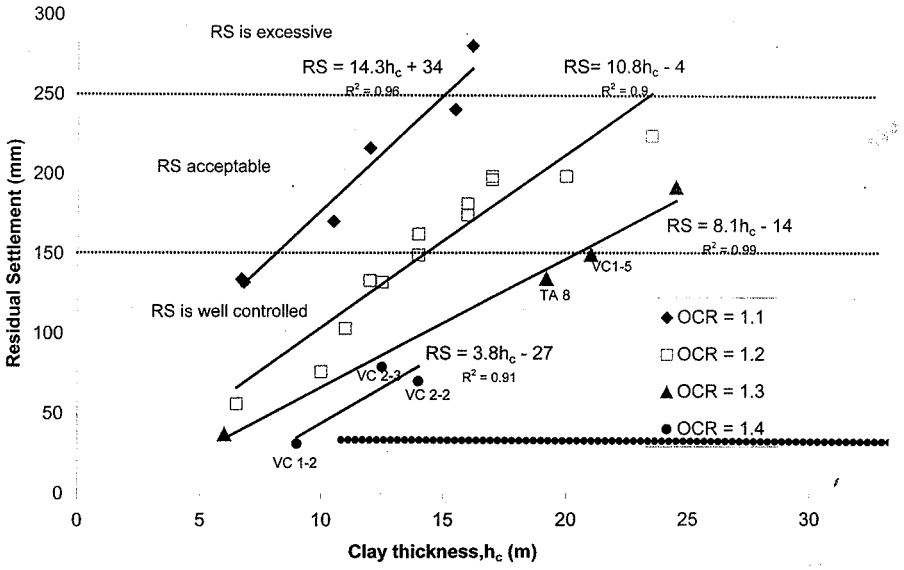

Figure 37: Effect of OCR and clay thickness on residual settlement.

6.2 BALLINA BYPASS

The Pacific Highway linking Sydney and Brisbane is constructed to reduce the high traffic congestion in Ballina. This bypass route has to cross a floodplain consisting of highly compressible and saturated marine clays up to 40 m thick. A system of vacuum assisted surcharge load in conjunction with PVDs was selected to shorten the consolidation time and stabilise the deeper clay layers. To investigate the effectiveness of this approach, a trial embankment was built north of Ballina, 34 mm diameter circular PVD at 1.0 m spacing were installed in a square pattern. The vacuum system consisted of PVDs with an air and watertight membrane, horizontal transmission pipes, and a heavy duty cacuum pump. Transmission pipes were laid horizontally beneath the membrane to provide uniform distribution of suction. The boundaries of the membrane were embedded in a peripheral trench filled with soil-bentonite to ensure absolute air tightness. Figure 38 presents the instrument locations, including surface settlement plates, inclinometers and piezometers. The piezometers were placed 1 m, 4.5 m, and 8 m below the ground level, and eight inclinometers were installed at the edges of each embankment. the embankment area are was then divided into Section A (no vacuum pressure), and Section B, subject to vacuum pressure and surcharge fill. As the layers of soft clay fluctuated between 7 m to 25 m (Table 2), the embankment varied from 4.3 m to 9.0 m high, to limit the post-construction settlement. A vacuum pressure of 70 kPa was applied at the drain interface and removed after 400 days. The geotechnical parameter of the three subsoil layers obtained from standard odometer tests are given in Table 3.

Table 2 Bottom level of soft clay layer at each settlement plate (Indraratna *et al.* 2009).

Settlement plate	SP1, SP2	SP3, SP4	SP5, SP6	SP7 SP8	SP9 SP10	SP11 SP12
Bottom level of soft clay layer (m-RL)	2.7-6.7	6.7-9.7	9.7-11.7	11.7-14.7	14.7-17.7	20.7-24.7

Table 3 Soil parameters at SP12 (Indraratna *et al.* 2009).

Depth (m)	**Soil Type**	λ	κ	γ **kN/m3**	e_0	$k_{h,ax}$ **10^{-10} m/s**	**OCR**
0.0-0.5	Clayey silt	0.57	0.06	14.5	2.9	10	2
0.5-15.0	Silty Clay	0.57	0.06	14.5	2.9	10	1.7
15.0-24.0	Stiffer Silty Clay	0.48	0.048	15.0	2.6	3.3	1.1

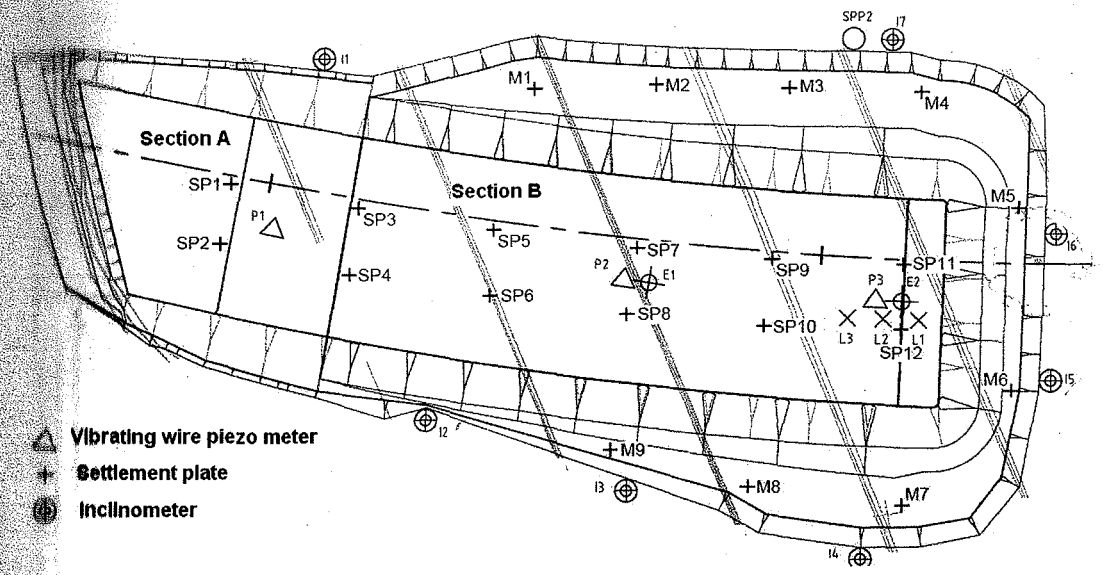

Figure 38: Instrumentation layout for the test embankments at Ballina Bypass (Indraratna *et al,*. 2009).

The soil profile with its relevant properties is shown in Fig. 39. A soft silty layer of clay approximately 10 m thick was underlain by a moderately stiff, silty layer clay located 10-30 m deep, which was in turn underlain by firm clay. The groundwater was almost at the ground surface. The water content of the soft and medium silty clay varied from 80 to 120%, which was generally at or exceeded the liquid limit, ensuring that the soils were fully saturated. The field vane shear tests indicated that the shear strength was from 5-40 kPa. The compression index ($C_c/(1+e_0)$) determined by standard oedometer testing was between 0.30-0.50.

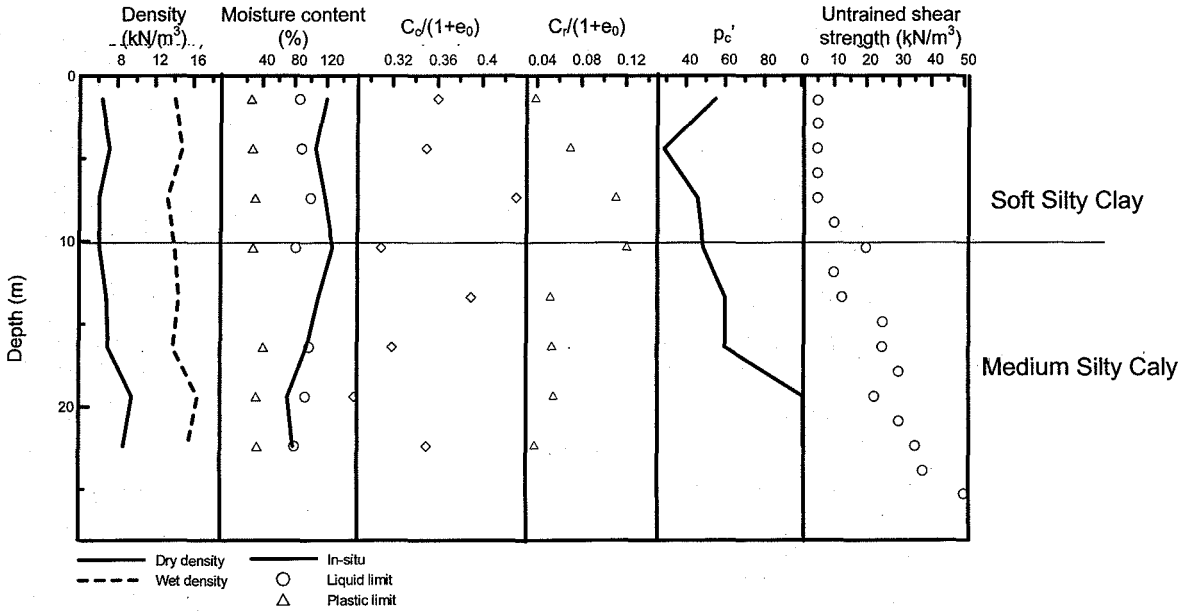

Figure 39: General soil profile and properties at Ballina Bypass (Indraratna *et al.*, 2009).

Settlement and associated pore pressure recorded by the settlement plates and piezometers are shown in Fig. 40, with the embankment construction schedule. The actual suction varied from -70 kPa to -80 kPa, and no air leaks were encountered. Suction was measured by miniature piezometers embedded inside the drains.

Lateral displacement at the border of the embankments needed to be examined carefully, particularly the vacuum area where the surcharge loading was raised faster than that at the non-vacuum area. The soil properties and lateral displacement plots before and after vacuum are shown in Fig. 41. Inclinometer I1 was installed at the border of the vacuum area, whereas inclinometers I2-I4 were located at the edge of the vacuum area. Here the lateral displacement subjected to vacuum were smaller even though the embankments were higher. In Figure 41b the plot of lateral displacement normalised to embankment height showed that the vacuum pressure undoubtedly reduced lateral displacement.

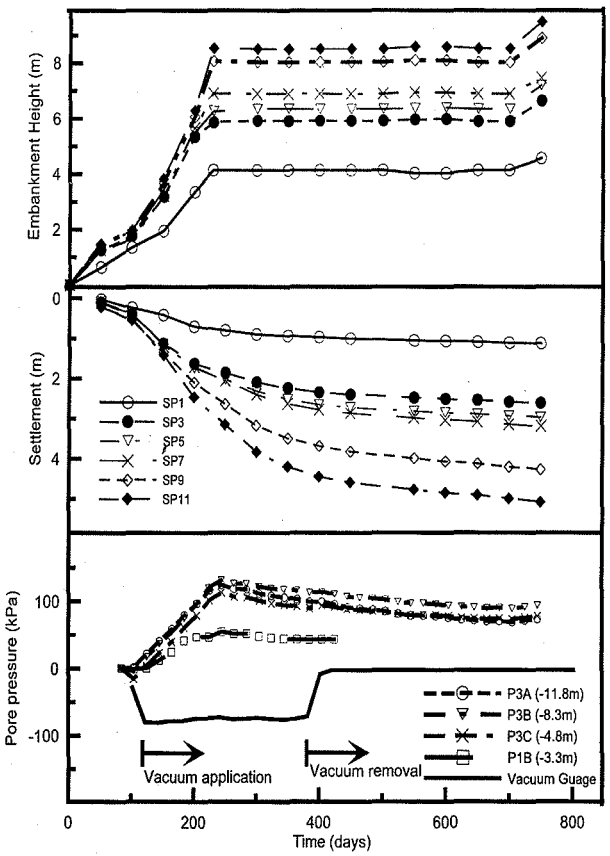

Figure 40: Embankment stage construction with associated settlements and excess pore pressures (Indraratna *et al.*, 2009).

2D and 3D single drain analyses were used to compute the settlement at location SP-12. Typical 2D finite element mesh are shown in Fig. 42a. The construction history and measured settlement at the settlement plate SP-12 are shown in Fig. 42b. Here the clay was assumed to 24 m thick, based on the CPT data. The analytical pattern was similar to Indraratna et al. (2005a). The predictions from 2D and 3D analyses agreed with the measured data, where the rate of settlement increased significantly after a vacuum was applied (Fig. 42c).

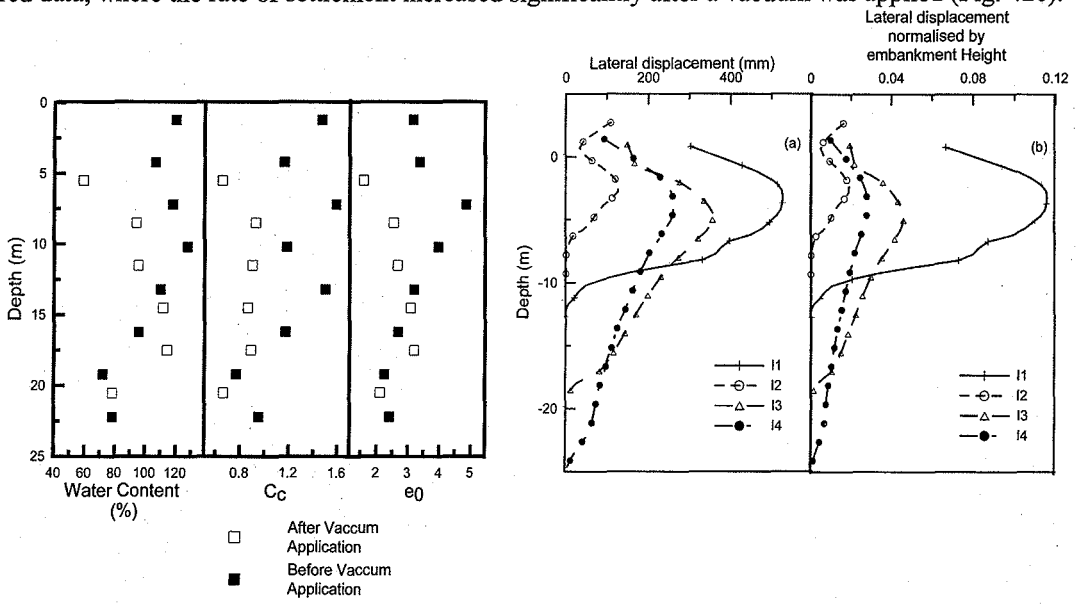

(a) (b)

Figure 41: (a) Soil properties before and after vacuum application; and (b) Measured lateral displacement and lateral displacement normalised with embankment height (Indraratna *et al.*, 2009).

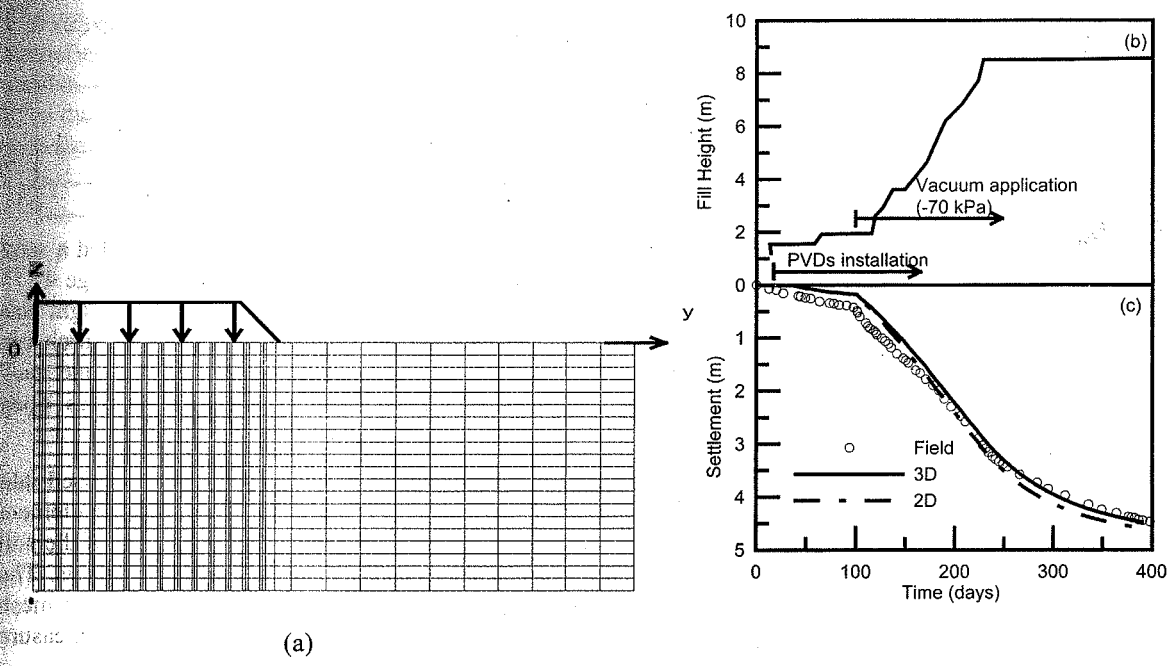

Figure 42: (a) 2D Finite element mesh; (b) loading history; and (c) consolidation settlements for settlement plate SP-12 (Indraratna *et al.,* 2009).

6.3 SECOND AIRPORT BANGKOK INTERNATIONAL AIRPORT

The Second Bangkok International Airport is located about 30 km east of Bangkok. The subsoil consists of a relatively uniform, top weathered crust (1.5 m thick). A stiff clay layer underlies the soft clay to a depth of 20-24 m below the ground surface. During the wet season, the area is often flooded and the soil generally retains a very high moisture content. The various sub-soils and pattern of the vertical drain are shown in Figure 43. Table 4 shows the geometric drain parameters and Table 5 gives the plane strain permeability coefficients (with and without smear) for Bangkok clay.

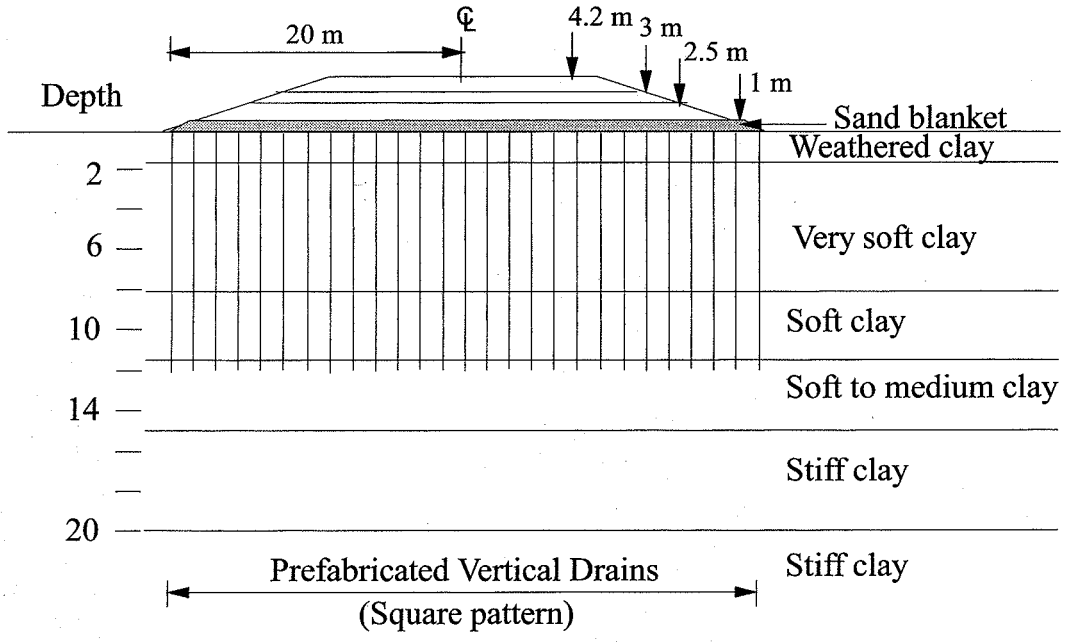

Figure 43: Cross section of an embankment with the subsoil profile, Second Bangkok International Airport, Thailand (Indraratna *et al.*, 2000).

Table 4: Geometric parameters of the drains for embankments TS1, TS2 and TS3 at Second Bangkok International Airport (Indraratna *et al,*. 2000).

Embankment	Spacing (m)	B (m)	b_w (m)	b_s (m)
TS1	1.5	0.75	0.03	0.27
TS2	1.2	0.60	0.03	0.27
TS3	1.0	0.50	0.03	0.27

The embankment load was applied in stages, whereby Stage 1 was equivalent to 18 kPa which included a sand blanket and clay sand 1.0 m high. Stage 2 was raised to 45 kPa, followed by Stage 3 (54 kPa) and Stage 4 (75 kPa), which gave a total fill height of 4.2 m. To maintain stability, a berm of 5 m width and 1.5 m height was added after the surcharge increased from 45 to 54 kPa. The berm was increased to 7 m wide when the surcharge load exceeded 54 kPa. Settlement and excess pore water pressure was monitored for over 1 year, and each embankment was monitored using settlement plates, slope inclinometers, and piezometers such as open standpipes and closed hydraulic piezometers.

The finite element mesh used in the embankment is shown in Fig. 44. The clay foundation was discretised into linear strain quadrilateral (LSQ) elements. A finer mesh was used for the PVD zone where each drain element represents a PVD containing the smear zone on either side of it (see insert, Fig. 44). The properties of the soil inside and outside the smear zone were assumed to be similar to those used in the single drain analysis. The instrumentation were placed in the mesh in such a way that so the measuring points coincided with the mesh nodes. The piezometers were placed 0.75 m from the centreline of the embankment between 2 drains, to measure the excess pore water pressure.

Table 5: Undisturbed and smear zone hydraulic conductivities for Bangkok clay and Muar clay (Indraratna *et al.* 2000).

Embank-ment	Depth (m)	k_h (m/s)	k_v (m/s)	k_{hp} (m/s) (no smear)	k'_{hp} (m/s) (with smear)
	0-2	5.23×10^{-8}	2.99×10^{-8}	1.47×10^{-8}	1.18×10^{-9}
TS1	2-7	1.2×10^{-8}	6.83×10^{-9}	3.36×10^{-9}	2.7×10^{-10}
(S=1.5 m)	7-12	5.25×10^{-9}	3.0×10^{-9}	1.48×10^{-9}	1.19×10^{-10}
	0-2	5.23×10^{-8}	2.99×10^{-8}	1.62×10^{-8}	2.04×10^{-9}
TS2	2-7	1.2×10^{-8}	6.83×10^{-9}	3.63×10^{-9}	4.67×10^{-10}
(S=1.2 m)	7-12	5.25×10^{-9}	3.0×10^{-9}	1.63×10^{-9}	2.05×10^{-10}
	0-2	5.23×10^{-8}	2.99×10^{-8}	1.78×10^{-8}	2.91×10^{-9}
TS3	2-7	1.2×10^{-8}	6.83×10^{-9}	4.05×10^{-9}	6.65×10^{-10}
(S=1 m)	7-12	5.25×10^{-9}	3.0×10^{-9}	1.78×10^{-9}	2.92×10^{-10}

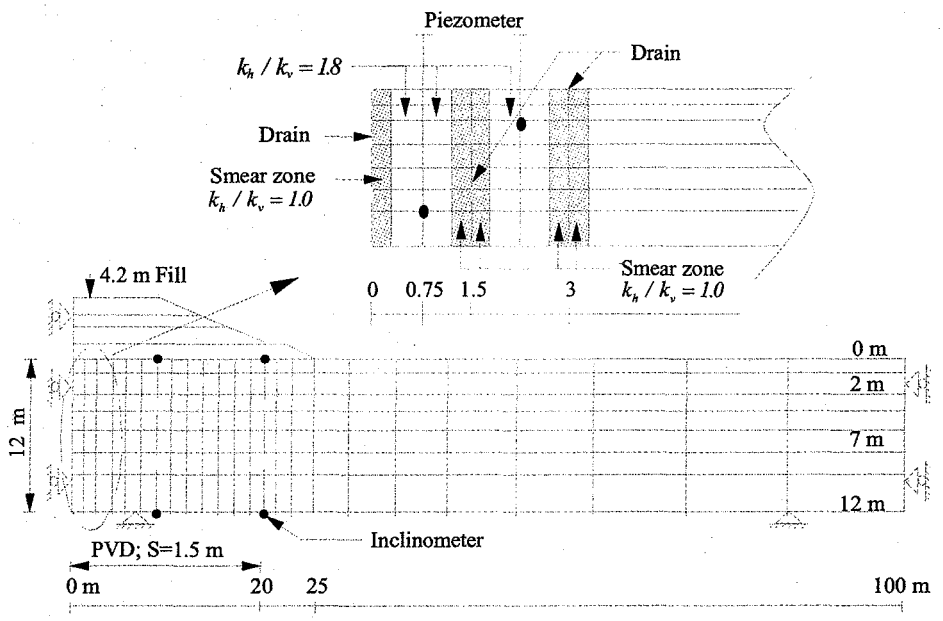

Figure 44: Finite element mesh of embankment for plane strain analysis at Second Bangkok International Airport (Indraratna *et al.*, 2000).

Ground settlement for the three embankments is shown in Figure 45, and the predictions were mode from the centreline of each embankment up to 100 m away. As shown, the predicted and measured settlement was very similar. Heave or swelling was predicted to take place past the toe of the embankment, i.e. about 27 m away from the centreline. Surface settlement was measured on either side of the centreline and proved to be acceptable with the calculated settlement profiles.

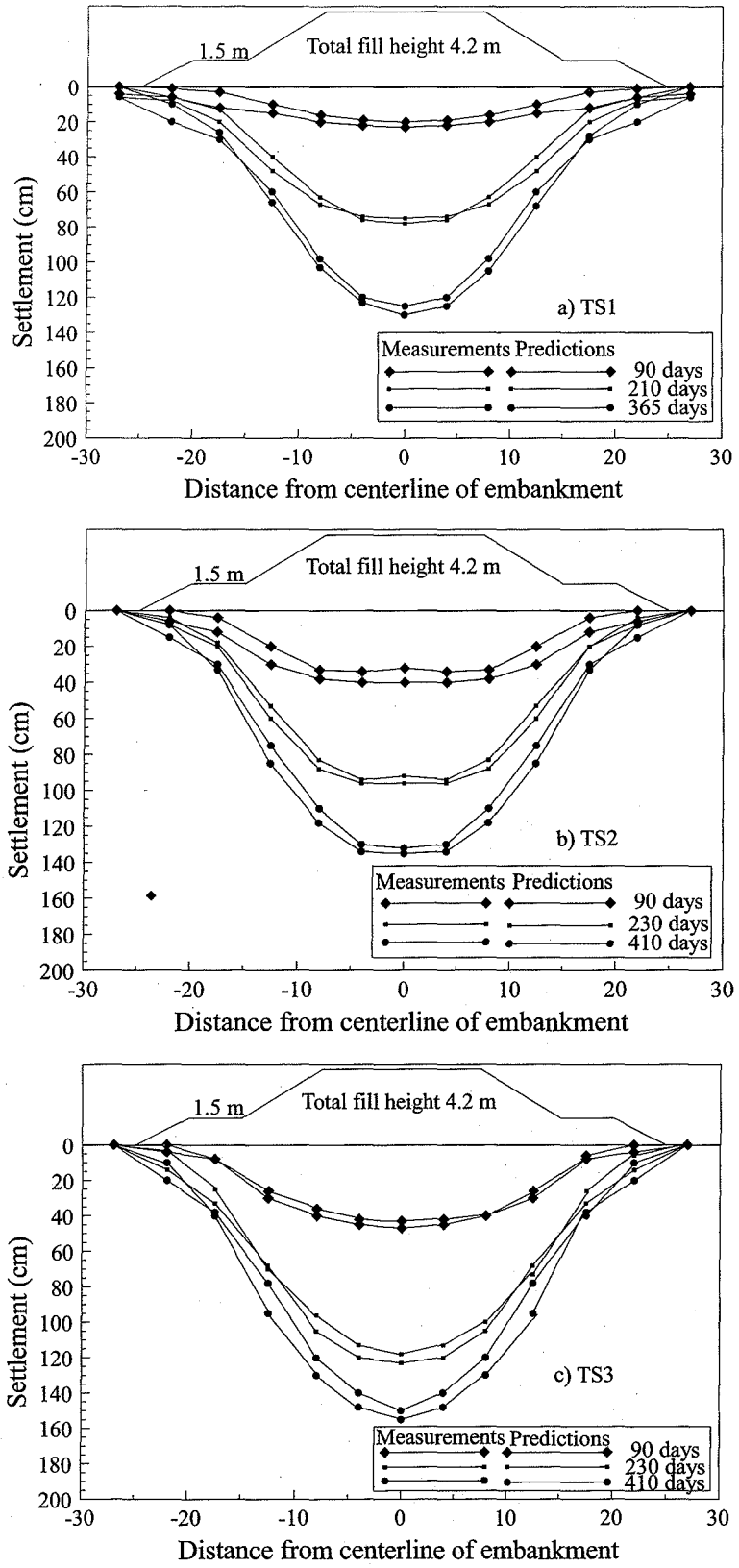

Figure 45: Surface settlement profile for embankments: a) TS1; b) TS2; and c) TS3, Second Bangkok International Airport (Indraratna *et al.*, 2000).

6.4 TIANJIN PORT

Tianjin port is approximately 100km from Beijing, China. The top 15 m of soil at this site was soft to very soft and needed to be improved using a preloading surcharge of more than 140 kPa (Rujikiatkamjorn *et al.*, 2008). To avoid any stability problems (high lateral yield) associated with a high surcharge embankment, a fill height of 50 kPa plus a vacuum pressure of 80 kPa was applied on top of the 20 m thick soft soil layer in construction with PVDs installed at 1.2 m spacing. The conversion method proposed by Indraratna *et al.* (2005b) was used for the 2D plane strain FEM analysis (Fig. 47), and the finite element program (ABAQUS) was used to simulate the 3D multi-drain analysis (Fig. 48), employing the Biot coupled consolidation theory.

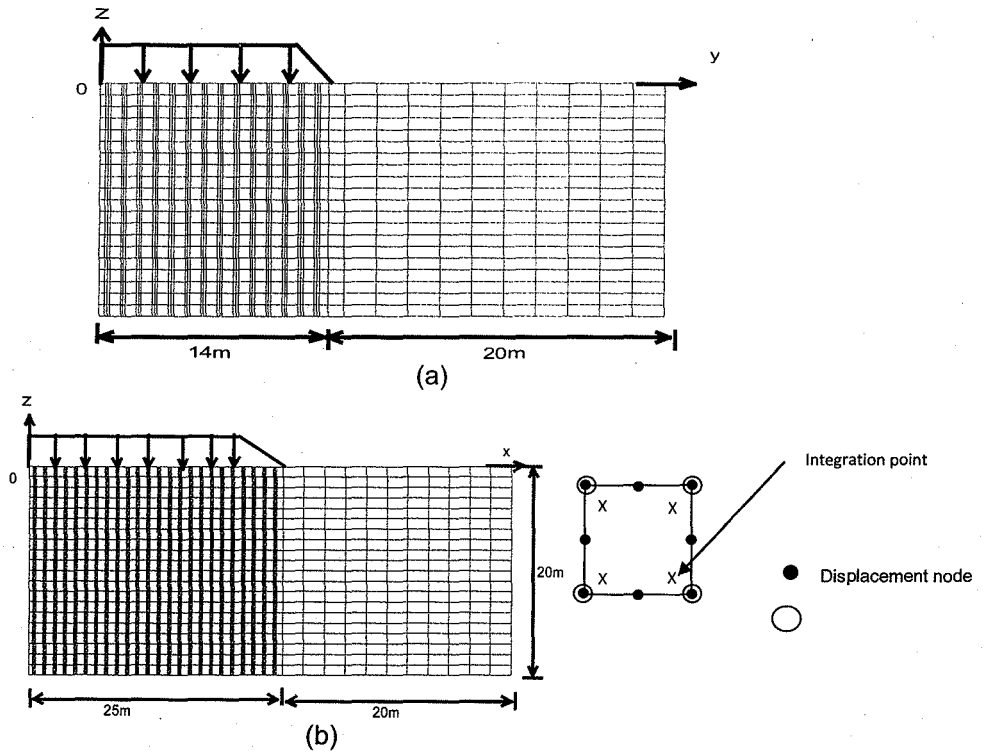

Figure 47: 2D finite-element mesh: (a) x=0 plane; (b) y=0 plane (Rujikiatkamjorn *et al.*, 2008).

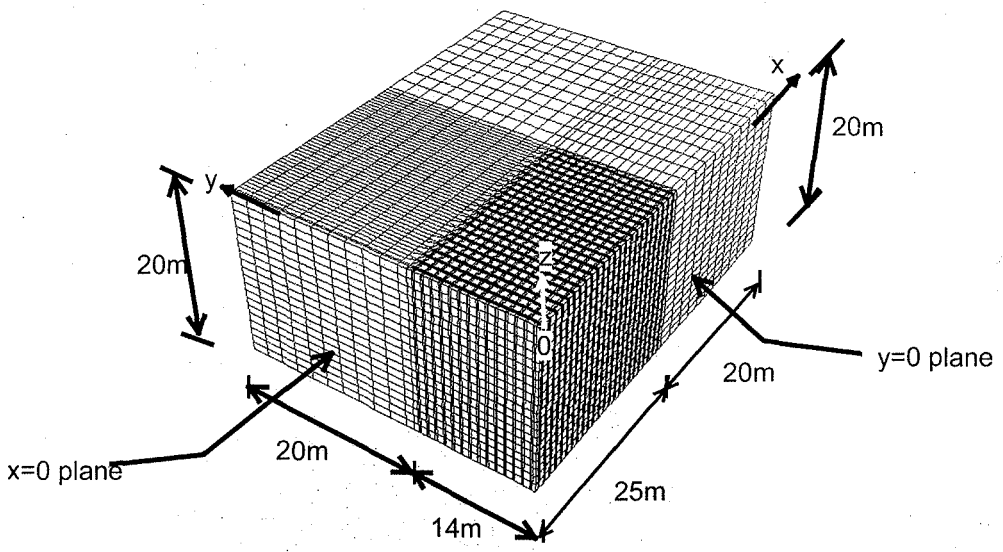

(a)

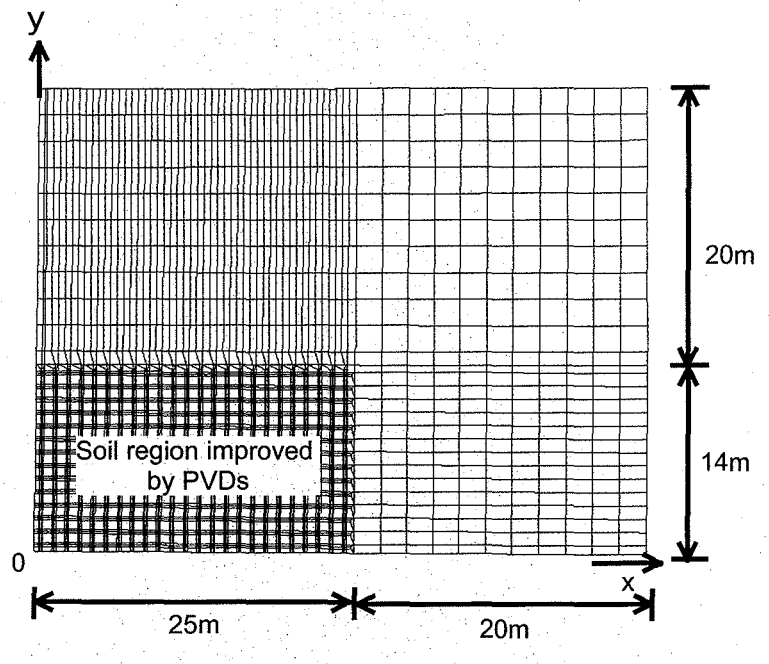

(b)

Figure 48: 3D finite-element mesh: (a) Isometric view; (b) top view (Rujikiatkamjorn *et al.,* 2008).

In terms of settlement, excess pore pressure, and lateral displacement, the numerical results from the equivalent 2D and true 3D analyses were quite similar (Figs. 49 and 50). This proves that, the equivalent plane strain (i.e. 2D) analysis was sufficient from a computational point of view, especially for multi-drain analysis of large projects where a 3D model would be more time consuming. From a practical point of view, the height of surcharge fill can be reduced by applying a vacuum preloading to achieve the same rate and degree of consolidation. Applying a surcharge pressure after the initial vacuum preloading could also reduce excessive inward lateral movement near the toe of the embankment (Rujikiatkamjorn *et al.,* 2008; Rujikiatkamjorn *et al.,* 2007).

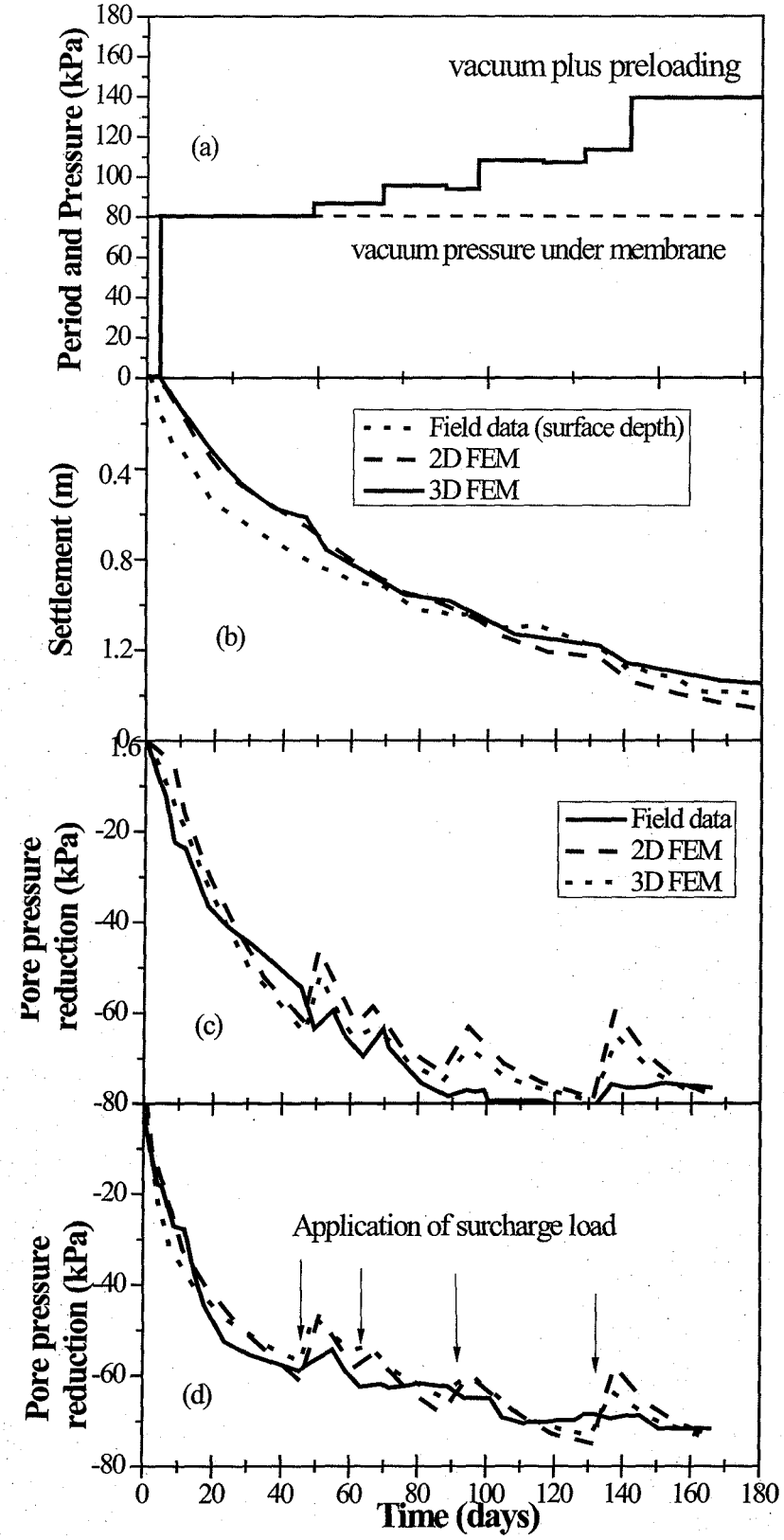

Figure 49: (a) Loading history; (b) consolidation settlements; (c) pore pressure variation at 0.25 m away from embankment centreline (Section II): 5.5 m depth; (d) pore pressure variation at 0.25m away from embankment centreline (Section II): 11.0 m depth (arrows indicate items when surcharge loads were applied) (Rujikiatkamjorn *et al.*, 2008).

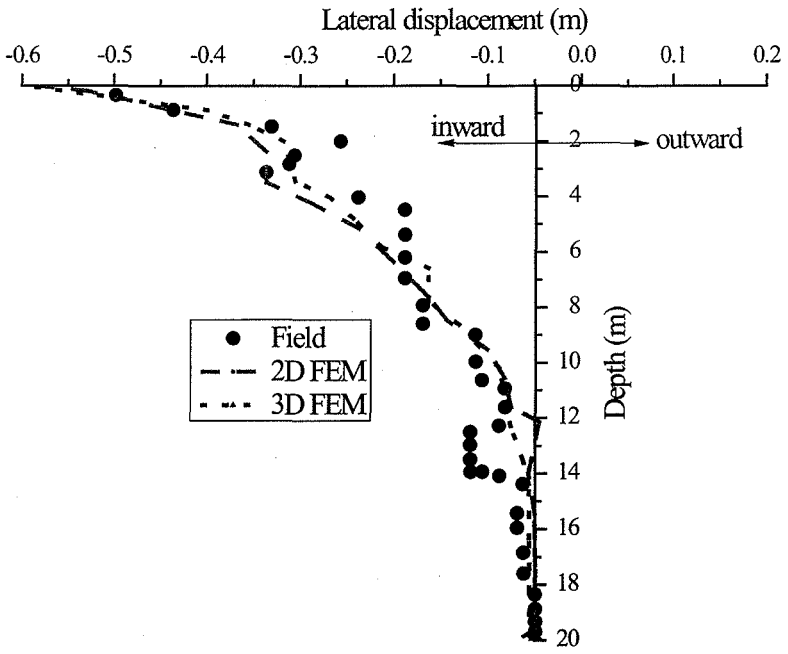

Figure 50: Lateral displacements at embankment toe (Section II at 180th day) (Rujikiatkamjorn *et al.*, 2008).

7 DESIGN CHARTS

7.1 DESIGN STEPS

Rujikiatkamjorn and Indraratna (2008) proposed design charts eliminating cumbersome iteration procedures using the equivalent drain diameter as an independent variable to obtain the relevant drain spacing. The design steps are summarised below:

1. Use the available soil profiles, in-situ test measurements and laboratory data to obtain the relevant soil properties, hence, determine the appropriate installation depth (l), and the desired consolidation time (t);

2. Assume the required degree of consolidation U_t for surcharge fill alone;

3. For vacuum pressure application, specify the mean suction, p_0, required total design stress $\Delta\sigma$, and the surcharge fill pressure, Δp and then determine the required degree of consolidation from $U_{t,vac} = (\Delta\sigma/(p_0 + \Delta p))^* U_t$

4. Use c_v, t and l, to determine u^* using Fig. 51 or from,

$$u^* = \sum_{m=1}^{\infty} \frac{8}{(2m+1)^2 \pi^2} \exp\left(-\left(\frac{2m+1}{2}\right)^2 \pi^2 T_v\right) \quad (17)$$

5. Determine the available size of the prefabricated vertical drains (circular or wick shape) and then compute the equivalent drain diameter (for wick drains), d_w from $d_w = 2(a+b)/\pi$;

6. Find T_h' from:

$$T_h' = c_h t / d_w^2 \quad (18)$$

7. Calculate $$\gamma = -\frac{8T_h'}{\ln\left(\frac{1-U_t}{u^*}\right)}$$ for surcharge fill only (no vacuum), (19)

or $$\gamma = -8T_h' / \ln\left(\frac{1-U_{t,vac}}{u^*}\right)$$ for vacuum pressure plus surcharge fill (20)

8. Establish the diameter and permeability of the smear zone;

9. Determine ξ using Fig. 52 or from the equation:

$$\xi = \left(\frac{k_h}{k_s} - 1\right)\ln(s) \quad (21)$$

10. Calculate n from $$n = \exp(\alpha \ln\gamma + \beta); \quad (22)$$

where, $$\alpha = 0.3938 - 9.505\times10^{-4}\xi^{1.5} + 0.03714\xi^{0.5} \quad (23a)$$

and $$\beta = 0.4203 + 1.456\times10^{-3}\xi^{2} - 0.5233\xi^{0.5}; \quad (23b)$$

11. Calculate the influence zone ($d_e = nd_w$);

12. Choose the drain pattern and determine the spacing of drain (d) from either $d = d_e/1.05$ (triangular grid) or $d = d_e/1.128$ (square grid).

7.2 WORKED-OUT EXAMPLE

The required soil parameters for the project are assumed to be: U_t = 90%, l = 24m, d_w = 34 mm (circular drain: Mebra-MCD34), c_h = 2.5 m^2/year, c_v = 1.0m^2/year, k_h/k_s = 5, s = 3, Maximum Design Surcharge, $\Delta\sigma$ = 120 kPa, surcharge fill pressure, Δp = 60 kPa, vacuum pressure, p_0 = -60kPa (suction). Well resistance is neglected. Calculate the drain spacing (d), for (a) t = 1.0 year; (b) t = 9 months; and (c) how the drain spacing can be altered with an increased vacuum pressure up to 90 kPa over 9 months.

Solution:

Part (a) t = 1.0 year

1. $T_v = 1.0\times1/24^2 = 0.002$; $U_{t,vac} = (120/(60+60))*0.9 = 0.9$

2. Calculate u^* using Equation **17** or from Fig. 51, hence, u^*= 0.95

3. $T_h' = c_h t/d_w^2 = 2.5\times1.0/0.034^2 = 2163$

4. $$\gamma = -\frac{8T_h'}{\ln\left(\frac{1-U_{t,vac}}{u^*}\right)} = -\frac{8\times2163}{\ln\left(\frac{1-0.9}{0.95}\right)} = 7686$$

5. From Fig. 52 or using Equation (**21**), $\xi = 4.39$

6. Using Equations (**23a & 23b**), determine $\alpha = 0.463$ and $\beta = -0.649$.

7. From Equation (**22**), $n = \exp(\alpha\ln\gamma + \beta) = \exp(0.463\times\ln 7686 - 0.649) = 33$

8. Calculate d_e from, $d_e = n\,d_w = 33\times0.034 = 1.122$ m

9. Drain spacing = 1.1 m for triangular (1.122/1.05) or 1.0 m for square grid (1.122/1.128), respectively.

The above calculations confirm that the design spacing of 1m×1m used at Ballina Bypass can be justified for similar soil properties.

Part (b) t = 0.75 years (9 months)

1. $T_v = 1.0\times0.75/24^2 = 0.001$; $U_{t,vac} = (120/(60+60))*0.9 = 0.9$

2. Calculate u^* using Equation 17 or from Fig. 51; hence, u^*= 0.96

3. $T_h' = c_h t/d_w^2 = 2.5\times0.75/0.034^2 = 1622$

4. $$\gamma = -\frac{8T_h'}{\ln\left(\frac{1-U_{t,vac}}{u^*}\right)} = -\frac{8\times1622}{\ln\left(\frac{1-0.9}{0.96}\right)} = 5737$$

5. Using Fig. 52 or from Equation (21), $\xi = 4.39$

6. From Equations (23a 7 23b), find $\alpha = 0.463$ and $\beta = -0.649$.

7. From Equation (**22**), $n = \exp(\alpha\ln\gamma + \beta) = \exp(0.463\times\ln 5737 - 0.649) = 29$

8. Calculate d_e from $d_e = n\,d_w = 29\times0.034 = 0.986$ m

9. Drain spacing = 0.95m for triangular grid (i.e. 0.986/1.05) or 0.90m for square grid (i.e. 0.986/1.128).

Part (c): Vacuum pressure increased up to 90 kPa over 9 months. Revised Drain Spacing?

1. $T_v = 1 \times 0.75/24^2 = 0.001$; $U_{t,vac} = (120/(90+60)) * 0.9 = 0.72$
2. Calculate u^* using Equation **17** or Fig. 51, Hence, $u^* = 0.96$
3. $T_h' = c_h t / d_w^2 = 2.5 \times 0.75 / 0.034^2 = 1622$
4. $$\gamma = -\frac{8T_h'}{\ln\left(\frac{1-U_{t,vac}}{u^*}\right)} = -\frac{8 \times 1622}{\ln\left(\frac{1-0.72}{0.96}\right)} = 10531$$
5. Use Fig. 52 or Equation (**21**), $\xi = 4.39$
6. Using Equations (**23a and 23b**), find $\alpha = 0.463$ and $\beta = -0.649$.
7. From Equation (**22**), $n = \exp(\alpha \ln \gamma + \beta) = \exp(0.463 \times \ln 10531 - 0.649) = 38$
8. Calculate d_e from $d_e = n\, d_w = 38 \times 0.034 = 1.29$ m
9. Drain spacing = 1.23m for triangular pattern (i.e. 1.29/1.05) or 1.14m for square grid (i.e.1.29/1.128).

This demonstrates that increased vacuum pressure allows the drain spacing to be increased. This should also reduce the risk smear overlapping and reduced drain costs.

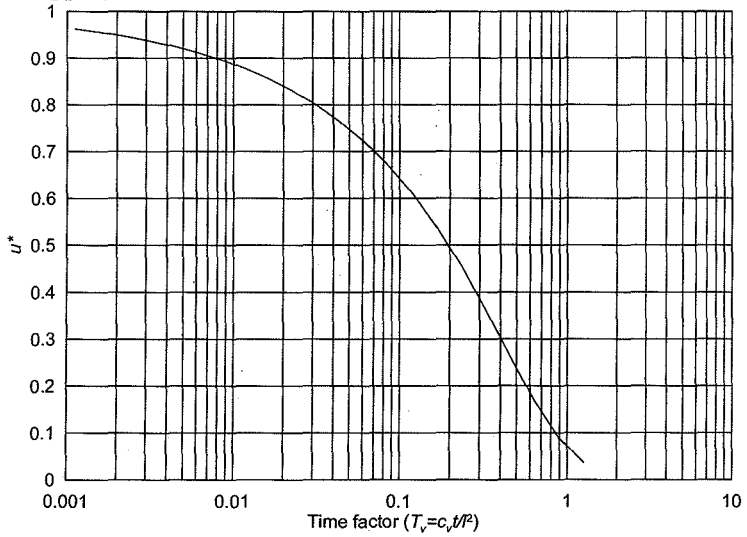

Figure 51: Relationship between T_v and u^* (Rujikiatkamjorn and Indraratna, 2007).

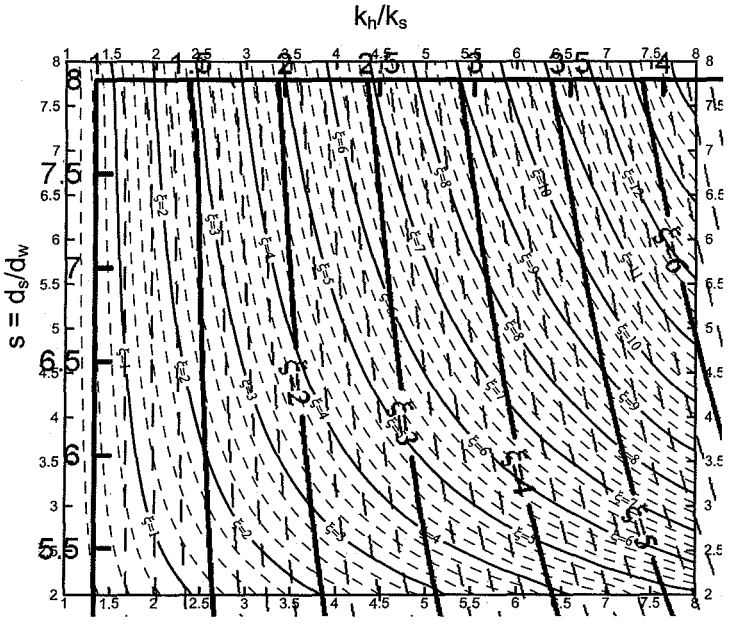

Figure 52: Contours of ξ based on Eq. (**19**) (Rujikiatkamjorn and Indraratna, 2007).

8 CONCLUSION

It is clear that the application of PVDs combined with vacuum and surcharge preloading has become common practice, and is now considered to be one of the most effective ground improvement techniques. Analytical and numerical modelling of vacuum preloading is still a developing research area. There has always been a discrepancy between the predictions and observed performance of embankments stabilised with vertical drains and vacuum pressure. This discrepancy can be attributed to numerous factors such as the uncertainty of soil properties, the effect of smear, inaccurate assumptions of soil behaviour and vacuum pressure distribution, and an improper conversion of axi-symmetric condition to plane strain (2D) analysis of multiply drains.

Vacuum assisted consolidation is an innovative method which has recently, and successfully, been used for large-scale projects on very soft soils in reclamation areas. The extent of surcharge fill can be decreased to achieve the same amount of settlement and the lateral yield of the soft soil can be controlled by PVDs used in conjunction with vacuum pressure. The effectiveness of this system depends on (a) the air tightness of the membrane, (b) the seal between the edges of the membrane and the ground surface, and (c) the soil conditions and location of the ground water level. The exact role of membrane type and membranless systems for vacuum preloading requires detailed evaluation. In the absence of a comprehensive and quantitative analysis, the study of suitable methods to apply vacuum preloading becomes imperative, experimentally, numerically and in the field.

To study the performance of vacuum assisted consolidation, a process simulation test using a large-scale consolidometer was conducted to obtain more realistic parameters, including the correct smear zone characteristics, the distribution of vacuum along the length of the drain, as well as soil and drain properties. Conventional small equipment (e.g. Rowe cell) cannot capture these parameters. The equivalent radius of the smear zone is generally 2-3 times larger than the equivalent radius of the mandrel and the soil permeability in the smear zone is lower than the undisturbed zone by a factor of 1.5-2. The presence of even a thin unsaturated layer of soil at the boundary of the PVD would retard the pore pressure dissipation at the initial stage of consolidation.

Analytical modelling of vertical drains that include vacuum preloading under axi-symmetric and plane strain conditions that simulate the consolidation of a unit cell surrounding a single vertical drain has been developed. The effects of vacuum propagation along the length of a drain and the occurrence of non-Darcian flow conditions have been incorporated in the proposed solutions to obtain a more realistic prediction. The elliptical cavity expansion theory provided further insight to evaluate the role that smear zone characteristics play on consolidation.

In large construction sites where many PVDs are installed, a 2D plane strain analysis is usually sufficient. The proposed conversion from axi-symmetric to a plane strain condition agreed with the data available from case histories, including Ballina Bypass and Port of Brisbane (Australia), the Second Bangkok International Airport (Thailand) and Tianjin Port (China). These simplified plane strain methods can be readily incorporated in numerical (FEM) analysis. The conversion procedure from 3D to 2D based on the correct transformation of permeability and vacuum pressure, ensure that the time-settlement curves are the same as the true 3D analysis. Field behaviour and model predictions indicate that the efficiency of vertical drains depends on the magnitude and distribution of vacuum pressure as well as the degree of drain saturation during installation, and the extent of smear caused by the vertically penetrating mandrel.

From a practical point of view, the surcharge fill can be reduced in height by using vacuum preloading to achieve the same desired rate of consolidation. This system eliminates the need for a high embankment surcharge load, but air leaks must be prevented as much as possible. Suitable design charts for vertical drains that consider both vertical and horizontal drainage have been developed. As a result, the conventional and often cumbersome trial and error methods used to estimate the appropiate parameters and spacing of drains be avoided. Once the equivalent drain diameter and other relevant parameters are known, the diameter of the influence zone can be readily obtained without any further iterations or interpolations. These preliminary design charts have now been extended to represent a larger array of soil properties and drain patterns, on the basis of the same governing equations presented here.

Apart from road embankments, PVDs will also help stabilise rail tracks in coastal areas containing a high percentage of clayey subgrades. It has been shown that short PVDs can be used under rail tracks to improve stability by dissipating excess cyclic pore pressure and curtailing lateral displacement. Much of this research is still ongoing at the University of Wollongong, particularly in view of future high speed rail. Current laboratory observations prove without doubt that high-speed trains cannot operate efficiently on tracks built on soft subgrade clays unless it is consolidated before construction, or alternative improvements such as chemical treatment or stone columns are considered.

9 ACKNOWLEDGEMENT

It has indeed been a great honour for me to accept the kind invitation from the Australian Geomechanics Society (AGS) to deliver the 2009 EH Davis Memorial Lecture. I am indebted to AGS and its local Chapters for hosting my presentation in all major cities. It is also my pleasure to present it in China and India at the invitation of the Geo-Shanghai and IGS Conference organisers, respectively.

I gratefully appreciate the help of Dr Geng Xueyu and Dr Cholachat Rujikiatkamjorn during compiling and editing of a vast amount of data from the past 15 years of research in vertical drains and vacuum preloading conducted at University of Wollongong (UOW). While it is impossible to include all the salient findings in a single publication, the 2009 E.H. Davis Lecture reflects a vital Australian contribution to soft soil improvement. At least a dozen PhD students, whom I have had the pleasure of supervising over the past 15 years, have contributed to the contents of this lecture as reflected by the cited references. In particular, I am indebted to Dr Wayan Redana (laboratory evaluation of smear effects), Dr Chamari Bamunawita (numerical modeling and laboratory assessment of vacuum pressure propagation), Dr Iyathurai Sathananthan (non-Darcian flow effects on radial consolidation), Dr Rohan Walker (influence of overlapping smear effects), and Dr Cholachat Rujikiatkamjorn (optimization of PVD and vacuum preloading in design).

A number of research projects on the application of vertical drains and vacuum preloading have been supported in the past and present by the Australian Research Council (ARC). I owe my gratitude to Mr Vasantha Wijeyakulasuriya, Director, Queensland Department of Main Roads (Brisbane) for his continuous support through several such projects over a decade. Indeed, the keen collaborations with industry through numerous projects have facilitated the application of theory to practice. In this respect, I sincerely thank Queensland Department of Main Roads, Port of Brisbane Corporation, Roads & Traffic Authority, Coffey Geotechnics, Polyfabrics, Geofabrics, ARUP, Douglas Partners, Snowy Mountains Engineering Corporation, RailCorp, ARTC, Chemstab, Queensland Rail and Austress-Menard.

The support and cooperation received at various times from many colleagues is gratefully appreciated. While it is impossible to name of all of them, special thanks are conveyed to Prof. Harry Poulos, Prof. (Bala) Balasubramaniam, Prof. Norbert Morgenstern, Prof. Chu Jian, Dr. Hadi Khabbaz, Dr. Jayantha Ameratunga, Prof. Sven Hansbo, Prof. Robin Chowdhury, Prof. Dennes Bergado, Dave Christie, Prof. Ted Brown, Prof. Serge Leroueil, Prof. Jian-hua Yin, Prof. Peter Kaiser, Dr. Richard Kelly, Patrick Wong, Prof. Chandra Desai, Peter Boyle, Assoc. Prof. (Siva) Sivakugan, Dr Brook Ewers, Henk Buys, Prof. Dave Potts, Geoff McIntosh, Prof. Gholamreza Mesri, Mark Adams, Prof. Scott Sloan, Prof. John Carter, Prof. Dave Chan, Prof Sarah Springman, Cynthia de Bok, Prof. Mohamed Sakr, Prof. Mounir Bouassida, Daniel Berthier, Prof. Mike Jamiolkowski, Prof. Pedro Pinto, Prof. Madira Madhav, Prof. Nasser Khalili, Prof. Jin-chun Chai, Dr Mohammad Shahin, Dr Gamini Adikari, Prof. Maosong Huang, Prof. Brian Uy, Dr Phil Flentje, Dr R. Robinson, Prof. Felix Darve, Julian Gerbino, Bob Armstrong, Michael Thomas, Dr. Deepankar Choudhury, Dr. Jayan Vinod, Dr Samanthika Liyanapathirana, Dr Martin Liu, Dr Sanjay Nimbalkar and Dr Lijun Su among others.

The support of University of Wollongong and its Faculty of Engineering had enabled me to foster productive soft clay engineering and ground improvement research programs under the Centre for Geomechanics & Railway Engineering. The dedication of its technical staff has been a key influential factor. Alan Grant, Ian Laird, Ian Bridge and Bob Rowlan have built in-house, most of the unique large-scale testing equipment used in ground improvement studies.

Much of the contents in the 2009 EH Davis Lecture are elaborated in numerous issues of the Canadian Geotechnical Journal, ASCE Journal of Geotechnical & Geoenvironmental Engineering, Geotechnique, ASCE J. of Geomechanics, Ground Improvement Case Histories, Elesevier (editors: by Indraratna & Chu) and several Keynote papers at international conferences. Selected contents from some of these articles were reproduced with kind permission.

Finally, without the support and understanding of my family, it would have been impossible to undertake and be successful in any research task that demands endless and passionate effort over time.

10 REFERENCES

Akagi, T. 1979. Consolidation caused by mandrel-driven sand drains. Proceedings of the 6th Asian Regional Conference on Soil Mechanics and Foundation Engineering, Singapore, Southeast Asian Geotechnical Society, Bangkok, Vol.1: 125–128.

Barron, R.A. 1948. Consolidation of fine-grained soils by drain wells. Transactions. ASCE, 113: 718-754.

Bergado, D.T. Bergado, H. Asakami, M.C. Alfaro and Balasubramaniam, A.S. 1991. Smear effects of vertical drains on soft Bangkok clay. J Geotech Eng, ASCE, 117(10): 1509–1530.

Bergado, D.T., Balasubramaniam, A.S., Fannin, R.J. and Holtz, R.D. 2002. Prefabricated vertical drains (PVDs) in soft Bangkok clay: a case study of the new Bangkok International Airport Project, Can Geotech J. 39: 304-315.

Bo, M.W., Chu, J., Low, B.K., and Choa, V. 2003. Soil improvement Prefabricated vertical drain techniques, Thomson Learning, Singapore.

Bjerrum, L. 1967. Engineering geology of Norwegian normall-consolidated marine clays as related to settlement of buildings, Geotechnique, 17(2): 73-96.

Chai, J.C., Cater, J.P., and Hayashi, S. 2005. Ground deformation induced by vacuum consolidation. J. Geotech. Geoenviron. Eng., 131(12): 1552-1561.

Chai, J.C., Miura, N., and Bergado, D.T. 2008. Preloading clayey deposit by vacuum pressure with cap-drain: Analyses versus performance. Geotextiles and Geomembranes. 26 (3) 220-230.

Choa, V. 1990. Soil improvement works at Tianjin East Pier project. Proceedings 10th Southeast Asian Geotechnical Conference, Taipei, 1: 47-52.

Chu, J., and Yan, S.W. 2005. Application of vacuum preloading method in soil improvement project. Case Histories Book, Edited by Indraratna, B. and Chu, J., Elsevier, London. Vol. 3: 91-118.

Chu, J., Yan, S. W., and Yang, H. 2000. Soil improvement by vacuum preloading method for an oil storage station. Geotechnique, 50(6): 625-632.

Gabr M.A. and Szabo D.J. 1997. Prefabricated vertical drains zone of influence under vacuum in clayey soil. Proceedings of the Conference on In Situ Remediation of the Geoenvironment, ASCE: 449-460.

Ghandeharioon, A., Indraratna, B., and Rujikiatkamjorn, C. 2010. Analysis of soil disturbance associated with mandrel-driven prefabricated vertical drains using an elliptical cavity expansion theory. Int. J. Geomech., 10 (2): 53-64

Hansbo, S. 1979. Consolidation of clay by band-shaped prefabricated drains. Ground Eng., 12(5): 16-25.

Hird C.C., Pyrah I.C., and Russel D. 1992. Finite element modeling of vertical drains beneath embankments on soft ground. Geotechnique, 42(3): 499-511.

Holtan, G.W. 1965. Vacuum stabilization of subsoil beneath runway extension at Philadelphai International Airport. In Proc. of 6th ICSMFE, 2.

Holtz, R.D., Jamiolkowski, M., Lancellotta, R. and Pedroni, S. 1991. Prefabricated vertical drains: design and performance, CIRIA ground engineering report: ground improvement. Butterworth-Heinemann Ltd, UK, 131 p.

Indraratna, B., Balasubramaniam, A. S. and Balachandran, S. 1992. Performance of test embankment constructed to failure on soft marine clay. J. Geotech. Eng., 118(1): 12-33.

Indraratna, B., Balasubramaniam, A. S., and Ratnayake, P. 1994. Performance of embankment stabilized with vertical drains on soft clay. J. Geotech. Eng., 120(2): 257-273.

Indraratna, B., and Redana, I. W. 1998. Laboratory determination of smear zone due to vertical drain installation. J. Geotech. Eng, 125(1): 96-99.

Indraratna, B., and Redana, I. W. 2000. Numerical modeling of vertical drains with smear and well resistance installed in soft clay. Can. Geotech. J., 37(1) 132-145.

Indraratna, B., Bamunawita, C., and Khabbaz, H. 2004. Numerical modeling of vacuum preloading and field applications. Can. Geotechech. J., 41(6) 1098-1110.

Indraratna, B., Rujikiatkamjorn C., and Sathananthan, I. 2005a. Analytical and numerical solutions for a single vertical drain including the effects of vacuum preloading. Can. Geotech. J., 42 (4): 994-1014.

Indraratna, B., Sathananthan, I., Rujikiatkamjorn C. and Balasubramaniam, A. S. 2005b. Analytical and numerical modelling of soft soil stabilized by PVD incorporating vacuum preloading. Int. J. Geomech., 5(2): 114-124.

Indraratna, B., Rujikiatkamjorn C., Balasubramaniam. A. S. and Wijeyakulasuriya, V. 2005c. Predictions and observations of soft clay foundations stabilized with geosynthetic drains vacuum surcharge. Ground Improvement – Case Histories Book Edited by Indraratna, B. and Chu, J., Elsevier, London: Vol 3:199-230.

Indraratna, B., and Rujikiatkamjorn, C. 2008. Effects of partially penetrating prefabricated vertical drains and loading patterns on vacuum consolidation. In K. R. Reddy, M. V. Khire & A. N. Alshawabkeh (Eds.), GeoCongress ASCE, USA :596-603.

Indraratna, B., Attya, A., and Rujikiatkamjorn, C. 2009a. Experimental investigation on effectiveness of a vertical drain under cyclic loads. J. Geotech. Geomenviron. Eng., ASCE. 135 (6), 835-839.

Indraratna, B., and Rujikiatkamjorn, C., Kelly, R., and Buys, H. 2009b. Soft soil foundation improved by vacuum and surcharge preloading at Ballina Bypass, Australia. International Symposium on Ground Improvement Technologies and Case Histories (ISGI09): 95-105

Indraratna, B., Rujikiatkamjorn, C. Adams, M., and Ewers, B., 2010. Class A prediction of the behaviour of soft estuarine soil foundation stabilised by short vertical drains beneath a rail track. J. Geotech. Geo-environ. Eng. ASCE (Accepted October 2009).

Jacob, A., Thevanayagam, S. and Kavazajian, E., 1994. Vacuum-assisted consolidation of a hydraulic landfill. Vertical and Horizontal Deformations of Foundations and Embankments, Settlement'94, College Station. ASCE Geotech. Sp. No 40, ASCE: 1249-1261.

Jamiolkowski, M., Lancellotta, R., and Wolski, W. 1983. Precompression and speeding up consolidation. Proc. 8th ECSMFE: 1201-1206.

Johnson, S. J., 1970. Precompression for improving foundation soils. J. Soil. Mech. Found. Div., 96 (1), 111-114.

Kjellman W. 1952, Consolidation of clayey soils by atmospheric pressure. Proceedings of a Conference on Soil Stabilisation, MIT, Boston: 258–263.

Mesri, G and Castro, A. 1987. The C_α / C_c concept and K_0 during secondary compression, J. Geotech. Eng. ASCE, 113(3): 230-247.

Mohamedelhassan E., and Shang, J.Q. 2002. Vacuum and surcharge combined one-dimensional consolidation of clay soils, Can. Geotech. J., 39 (5): 1126-1138.

Onoue, A. 1988. Consolidation by vertical drains taking well resistance and smear into consideration. Soils and Foundations, 28(4), 165-174.

Port of Brisbane Corporation and Austress Menard (2008), personal communication internal report and confidential. 79.

Qiun, J.H., Zhao, W.B., Cheung, Y.K. and Lee, P.K.K. 1992. The theory and practice of vacuum preloading. Comput. Geotech., 13 (2): 103-118.

Richart F.E. 1957. A review of the theories for sand drains. J. Soil Mech. Found. Div., 83(3): 1-38,

Roscoe, K.H., and Burland, J.B. 1968. On the generalized stress strain behavior of wet clay. Engineering Plasticity, Cambridge University Press; Cambridge, U.K.:535-609.

Rujikiatkamjorn, C., Indraratna, B. N. and Chu, J. 2008. 2D and 3D numerical modeling of combined surcharge and vacuum preloading with vertical drains. Int. J. Geomech., 8(2): 144-156.

Rujikiatkamjorn, C., Indraratna, B. 2007. Analytical solutions and design curves for vacuum-assisted consolidation with both vertical and horizontal drainage, Can. Geotech. J. 44 (2) :188-200.

Sathananthan, I. and Indraratna, B. 2006a. Laboratory evaluation of smear zone and correlation between permeability and moisture content. J. Geotech. Geoenviron. Eng., 132(7): 1090-0241.

Sathananthan, I. and Indraratna, B. 2006b. Plane-strain lateral consolidation with non-Darcian flow. Can. Geotech. J. 43 (2): 119-133.

Sathananthan, I., Indraratna, B. N. and Rujikiatkamjorn, C. 2008. Evaluation of smear zone extent surrounding mandrel driven vertical drains using the cavity expansion theory. Int. J. Geomech., 8 (6): 355-365.

Saye, S. R. 2001. Assessment of soil disturbance by the installation of displacement sand drains and prefabricated vertical drains. Soil Behaviour and Soft Ground Construction, ASCE, Geotech. Sp. No. 119: 325-362.

Seah, T.H. 2006. Design and construction of ground improvement works at Suvarnabhumi Airport". Geot. Eng, J. SE Asian Geotech. Society, 37: 171-188.

Walker, R. and Indraratna, B. 2006. Vertical drain consolidation with parabolic distribution of permeability in smear zone. J. Geotech. Geoenviron. Eng. 132(7), 937-941.

Walker, R. and Indraratna, B. 2007. Vertical drain consolidation with overlapping smear zones. Geotechnique, 57 (5): 463-467.

Yan, S.W. and Chu, J. 2003. Soil improvement for a road using a vacuum preloading method. Ground Improvement,7(4): 165-172.

Yin, J. H. and Clark, J. I. 1994. One-dimensional time dependent stress-strain behaviour of soils, elastic visco-plastic modelling, and consolidation analysis (Part 1). J. Rock Soil Mech., Chinese Academy of Sciences, 15(3): 65-80, (in Chinese). Part 2 on 15(4): 65-75 (in Chinese)